Diffusive Transport and Reaction in Clay Rocks: A Storage (Nuclear Waste, CO_2, H_2), Energy (Shale Gas) and Water Quality Issue

Laurent Charlet[1], Peter Alt-Epping[2], Paul Wersin[2] and Benjamin Gilbert[1,3]

[1] University Grenoble Alps**,** Earth Science Institute (ISTerre), F 38058 Grenoble, France.

[2] University of Bern, Institute of Geological Sciences, CH-3012 Bern, Switzerland.

[3] Energy Geosciences Division, Lawrence Berkeley National Lab, MS 74R316C, 1 Cyclotron Road, Berkeley CA 94720, USA

.

Table of Contents

Abstract

Clay rocks are low permeability sedimentary formations that provide records of Earth history, influence the quality of water resources, and that are increasingly used for the extraction or storage of energy resources and the sequestration of waste materials. Informed use of clay rock formations to achieve low-carbon or carbon-free energy goals requires the ability to predict the rates of diffusive transport processes for chemically diverse dissolved and gaseous species over periods up to thousands of years. We survey the composition, properties and uses of clay rock and summarize fundamental science challenges in developing confident conceptual and quantitative gas and solute transport models.

1. Introduction

Clay-rich (argillaceous) rocks, including marls, shale, mudstone, argillite and claystone (herein referred to as clay rocks), are sedimentary formations with a very low permeability for fluid flow. The low permeability of clay rock is a consequence of the nanoscale porosity of consolidated fine-grained sediments and may also be due to the loss of pore connectivity during diagenetic or metamorphic rock reactions. In addition, when two poorly miscible fluids such as

water and oil are present within a clay rock, the high capillary pressure at narrow pore throats can shut down the mobility of the non-wetting phase.

In the absence of significant fluid flow, diffusive transport mechanisms dominate. There is abundant evidence that the rate at which marine sediments attain geochemical equilibrium with an adjacent aquifer subjected to freshwater recharge, or the drop off in the productivity of a shale gas reservoir, are governed by very slow rates of diffusion through nanoporous clay rock. Understanding the pathways and mechanisms of solute and gas diffusion through clay rock is a critical objective for managing and utilizing the resources offered by these formations. In Section 1, we survey the uses of clay rock and the importance of understanding diffusive transport.

Macroscopic modeling to understand or anticipate long-term processes such as the geologic evolution of a formation or the shale gas production of a reservoir requires verified models of transport processes. These models will be improved by the development of more accurate descriptions of transport pathways and mechanisms, which remains very challenging for clay rock. In Section 2, we describe typical composition and structure of clay rock and devote considerable space to reviewing state-of-the-art approaches that are beginning to resolve the forms and connectivity of nanoscale pore networks.

Current models of diffusive transport average over all the molecular-scale interactions and processes that influence solute and gas transport. For example, the exclusion of anions from pores and interlayers formed by negatively charged clay mineral surfaces is typically accounted for by species-dependent geometric factors. Moreover, accounting for gas sorption by organic matter and clay minerals is an essential component for predicting gas capacity and transport, but is typically empirically determined for a given clay rock. Improved conceptual and quantitative models for gas and solute interactions with clay rock components will lead to more reliable connections between clay rock composition, structure and transport. In Section 3 we provide simplified descriptions of diffusive solute and gas transport and summarize efforts to link molecular and macroscale dynamics. In Section 4 we show how our current models of solute transport through clay rock can quantify millennial scale diffusive fluxes of tracers through sedimentary formations that are candidate locations for the storage of nuclear waste. The data and modeling provide compelling evidence for the exceptional sealing ability of these formations.

Virtually all uses of clay rock formations rely on their ability to prevent the transport of chemically reactive species, not only tracer ions. Carbon dioxide, hydrogen gas and redox sensitive elements can participate in diverse sorption, reaction, precipitation and dissolution processes that can significantly alter their mobility and in some cases can threaten the integrity of the clay rock. A major current challenge for the informed and sustainable use of clay rock systems is to develop improved understanding and models for diffusion coupled with reaction. In Section 5 we survey knowledge about reaction and retardation processes for a range of important species. This review cannot be a complete survey of clay rock processes but seeks to introduce common challenges and state-of-the-art approaches for a range of scientific communities.

The Contribution of Gary Sposito

Although the complexity of clay rock provides a severe challenge for mechanistic descriptions, the prolific career of Garrison Sposito exemplifies the approaches required for progress. He has conducted work at both the molecular and macroscopic levels, careful to differentiate mechanisms obtained at different timescales by different spectroscopic studies (see Sposito and Prost, 1982 [1]). Among hundreds of publications, many have provided key insight to processes controlling diffusion in clay rocks. He has pioneered studies of the structure and dynamics of water and ions in clays [2-4], and described mechanisms of ion and gas sorption onto clay minerals and organic matter [5, 6]. And he has reviewed, conceptualize and synthesized relevant work producing now standard textbooks in clay and soil science [7, 8].

1.1 Uses of Clay Rock

Radioactive Waste Storage

Storage of radioactive waste in deep geological formations is generally reserved for medium to high activities (quantities) of long-half-life radioisotopes. The vast majority of these waste types are generated by the nuclear fuel cycle, principally in the form of spent fuel and a variety of other waste types issuing from the reprocessing cycle including vitrified and bituminous waste. The safe and permanent geological storage of nuclear waste requires the waste to be stored in a storage complex that has low water permeability, reducing environment, high heat conductivity

and self-sealing properties in order to attenuate solute and gas transport. Deep geological disposal concepts are all based on placing the waste packages in specifically engineered facilities located deep underground (below 200 m depth) in carefully chosen geological contexts.

The clay rock formations currently under investigation as potential host formations for deep underground disposal facilities for radioactive waste include Boom Clay (Belgium and The Netherlands), Ypresian clay (Belgium), Boda Claystone (Hungary), Opalinus Clay (Switzerland), Callovo–Oxfordian argillite ("COx", France), Ordovician Cobourg argillaceous limestone (Canada) and diatomaceous mudstone at Horonobe (Japan). In such low permeability clay-rich rocks, solute migration will be mainly controlled by diffusion and sorption processes. The understanding of the migration processes and the determination of transport parameters for weakly or non-sorbing anionic radionuclides are of critical importance for the performance assessment of a deep geological repository [9, 10].

Gas transport processes are also critical for safe nuclear waste storage [11, 12]. Mechanisms leading to the formation of gas include the anaerobic corrosion of metals (forming H_2), the degradation of organic matter (CH_4, CO_2), radiolysis (H_2, O_2, CO_2, CH_4), steam generation near a spent fuel canister, helium production due to alpha decay and the release of radioactive gases (e.g. Rn). Gas generation may continue for long periods of time leading to a risk of overpressurizing and fracturing the surrounding clay rock unless it diffuses away, reacts with or sorbs on clay rock constituents [11].

Shale Gas Exploitation

In conventional fossil fuel reserves, an impermeable cap rock confines a hydrocarbon within a higher permeability reservoir. Nanoporous shales can themselves be long-term traps for oil and natural gas, but extraction from such unconventional resources was impractical until recently. Technological progress, in particular the combination of horizontal drilling with multiple stages of hydraulic fracturing, has enabled the dramatic development of unconventional hydrocarbon resources in the US [13]. Methane in shales is released by fracturing with pressurized water to create pathways for advective transport and using chemicals and sand to preserve fracture permeability (see, *e.g.*, Gregory *et al.*, 2011 [14]). The production of methane from fracked reservoirs follows a typical curve that can be modeled using direct numerical simulation of gas

flow through experimentally derived shale models [15] or semi-empirical theories of molecular transport in fractured nanoporous shale [16]. However, despite success by energy companies to identify geologic features of high yield shale plays and optimal extraction methods, we lack a complete fundamental understanding of the links between shale composition, structure and transport processes. This lack of understanding has direct environmental consequences. First, the very low efficiency of shale gas extraction has led to high drilling intensity with attendant risks of environmental impacts from surface operations and increased potential for well casing failure [17, 18]. Second, the management of water is critically important. While much fracking fluid is recovered, permanent water loss within a reservoir and salt or contaminant extraction can prevent reuse. Improved control of the release of contaminants within the formation, such as barium, radium or selenium, would reduce the toxicity of the flowback waters. Finally, shale gas extraction may release associated hydrocarbons such as ethane [19].

Geologic Carbon Storage

Geologic carbon storage (GCS) is identified by the IPCC as a necessary and urgent approach for lowering anthropogenic emissions of CO_2 to the atmosphere [20, 21]. High permeability saline aquifers or depleted oil and gas reservoirs overlain by low permeability sealing strata have a proven ability to host fluids over long timescales and recent trials at GCS sites have demonstrated the trapping of buoyant plumes of supercritical CO_2 [22-24]. The so-called stratigraphic trapping properties of caprock can be achieved by several types of low-permeability lithographies [25] including the fine-grain and carbonate-cemented sandstone at the depleted oil reservoir at Cranfield, Illinois (USA) [26]. However, laboratory and field studies suggest clay rock may have superior cap rock properties. Clay-rock reactions with low-pH carbonated brines are less likely to open new flow pathways (*e.g.*, through carbonate dissolution) and clay rock is more likely to self-seal should CO_2 injection pressures lead to the opening of new or pre-existing fractures [27]. Clay rock also forms a barrier for the transport of contaminants mobilized by CO_2 injection. At the Eau Claire, Illinois, an active GCS site [28], and at Green River, Utah (USA), a geologic analog for sequestered CO_2 [29], low-pH brines in the aquifer dissolved mineral phases such as iron oxides mobilizing incorporated or adsorbed contaminant ions such as selenite.

Hydrogen Storage or Release

A critical barrier for the greater penetration of renewables into electricity markets is the difficulty of storing energy from intermittent sources over long (multi-day and seasonal) time scales. The generation of hydrogen (H_2) by the electrolysis of water is a demonstrated approach for the utilization of excess electricity from renewables. In several European cities, H_2 from wind farms is added to the natural gas distribution network. However, if the H_2 can be stored, subsequent recombination with O_2 in air using a fuel cell will generate electricity that can be returned to the grid [30]. Commercial underground hydrogen storage (UHS) in salt caverns has been implemented in the US and UK for decades [31]. Alternative geological formations expected to be suitable for UHS include brine aquifers and depleted natural gas reservoirs [32]. There is growing evidence that H_2 could be effectively trapped by low permeability clay rock, increasing the potential geographic locations for UHS [33]. The requirements for a H_2 storage caprock are thus clearly different from clay-rich barriers proposed for radioactive waste sites that must prevent radionuclide migration while allowing repository gases to escape.

Shale Weathering

Shale weathering comprises a network of biogeochemical reactions that is driven by the exposure of reduced, organic-rich sedimentary clay rocks to O_2 and CO_2 [34]. Shale reactions may account for up to 40% of the global annual consumption of CO_2 through weathering of silicate and carbonate minerals [35]. Shale weathering causes coastal erosion, particularly around the UK and the arctic ocean, and can cause a significant input of contaminants, nutrients and salinity into terrestrial ecosystems. Clay rocks typically contain a range of minority elements or fluids that can negatively affect ecosystems if they are released through natural weathering processes or human activities. For example, the Mancos shale in the US has been identified as a source of contaminant metals and radionuclides including selenium and uranium [36]. Clay rocks can be reservoirs of geologic nitrogen including nitrate, ammonium stored in smectite interlayers and organic nitrogen compounds that could perturb the primary productivity of nitrogen-limited systems [37].

1.2 Geological Significance of Clay Rock

Records of Earth's evolutionary history

Shale beds have preserved a remarkable range of fossils including not only hard body parts but soft tissues, feathers, prints, and burrows. The cultural impact of these fossils, and their interpretation in terms of the history of life on Earth has been profound, including inspiring Darwin's theory of evolution. The accurate interpretation of large fossil skeletons began with Mary Anning along the coast of Lyme Regis (UK). Her discovery and re-assembly of a complete skeleton of an ichthyosaurus overturned the prevailing view that species were permanent and did not go extinct. Clay-rich sediments have preserved remarkable creatures from the Cambrian explosion at the Burgess Shale (Canada) [38] and feathered avians found in the Huajiying Formation (China) [39, 40]. Clay-rich sediments at Happisburgh, on the East coast of the UK, preserved the oldest known hominin footprints outside Africa at 0.78–1 Ma [41] informing our understanding of the colonization of Europe by human ancestors. All activities that access and manipulate surface and subsurface clay rock have the potential for making new discoveries about Earth history or destroying them forever. Properly coordinated subsurface research activities could facilitate access to new records of life on this planet. Knowledge of biological inputs and geologic processing has long been key for assessing potential oil and gas resources and we anticipate that similar perspectives will be required for all uses of clay rock. Because inorganic and organic fossils can significantly affect the porosity, geomechanics and reactivity of sedimentary rocks, explicit consideration of the biological inputs of clay rock will inform their planned uses.

Clay rock paleoredox trace element proxies

Clay rock can contain many trace elements in both organic and mineral phases that can provide valuable signatures of the origin and history of the sedimentary formation and that affect the use of clay rocks as a subsurface resource. For example, metals such as uranium, molybdenum and selenium are paleoredox indicators, as they are insoluble in their reduced oxidation state. Patterns of selenium isotopes may record cycles of oxidation and reductive processes, shedding light into past biogechemical regimes [42, 43]. Another paleoindicator is the presence of large amounts of Ba^{2+} in Marcellus formation clay interlayers [44]. These clays sedimented while the

Atlantic Ocean was opening and was still anoxic. As a consequence, inorganic sulfur was not yet oxidized as sulfate ions, as in modern ocean, allowing significant concentrations of barium ions to build up, and to be adsorbed on clays as exchangeable cations.

2. Clay rock composition and mechanical and hydraulic properties

Clay rocks originate from the deposition of argillaceous sediments in an aqueous (generally marine) environment. The Black Sea is a contemporary analogue of the environment in which carbonaceous shales and petroleum source beds formed [45]. Burial leads to the expulsion of the interstitial water, a strong decrease of porosity and increase in anisotropy [46]. During the consolidation process, diagenetic processes, including the formation of minerals (carbonates, sulfides), mineral transformations of clays (*e.g*. the smectite-to-illite reaction), and maturation of organic matter induces cementation that further reduces porosity [47]. Tectonic imprints include faulting and vein formation, uplift and erosion. An extensive nomenclature is employed for clay rocks to encompass the many different inputs and diagenetic processes, although no common descriptive vocabulary has been established [48].

2.1 Mineral composition

The mineralogy of clay rock is dominated by three major types: clay-calcite-quartz (and/or feldspar). Figure 1 shows that these minerals are found in considerably different proportions in shale, argillite, Boom and Opalinus Clays, argillaceous limestone, (*e.g*. the COx, described below) and also within these formations depending on depth. Minor components include sulfides (pyrite) and carbonates (dolomite, siderite) (see *e.g*.[49]). Some low-permeability sedimentary rocks contain relatively little clay, for example, the Koetoi and Wakkanai formations at Horonobe in Japan, a future HRW site, contain abundant fine-grained silicates derived from diatoms that confer very low permeability [50].

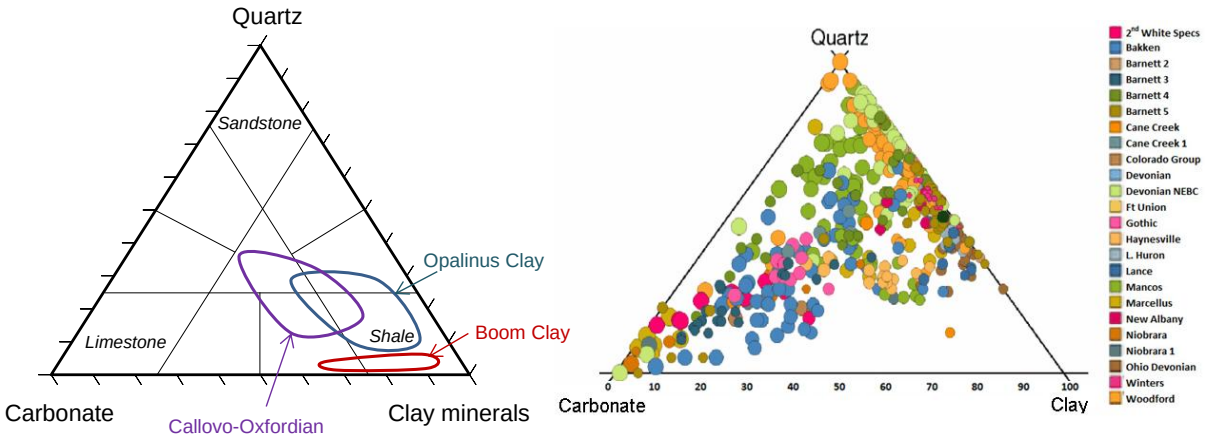

***Figure 1**: Ternary clay-quartz-carbonate plots demarking the clay rocks that are (a) currently under evaluation for radioactive waste storage (modified from [10]) and (b) active gas-bearing shales (modified from [51, 52]). A higher clay content favours fracture self-sealing and makes hydraulic fracturing more difficult.*

Clay minerals

The presence of layer silicate minerals, including clays and micas, is a key property of almost all low permeability sedimentary formations. Thorough characterization and identification of clay minerals have been carried out by complementary methods [53, 54]. The most common aluminosilicates include dominantly detrital clay minerals (illite, interstratified illite-smectite, chlorite and traces of kaolinite), minor detrital micas (biotite, muscovite), scarce detrital tourmaline and local diagenetic glauconite. Following burial, the conversion of swelling smectite to non-swelling illite is a common diagenetic process that releases silica that may precipitate as quartz that alters pore structure and mechanical properties [55].

Layer silicates are composed of sheets of silica tetrahedra and alumina octahedra in a 1:1 or 2:1 ratio separated by interlayer cations. We currently lack experimentally verified models for the distribution of metal substitutions within clay layers and the termination sites at clay edges. As will be discussed in the section "Sorption and retardation in clay rock", clay interlayer space can host exchangeable cations [56], while clay edges provide important sites for adsorption of metallic cations (*e.g.* Ni^{2+}, Cs^{+}), lanthanides or actinides as a function of *p*H [57-59].

The silica basal planes are terminated by siloxane groups and the hydrophobicity/hydrophilicity of clay and mica basal surfaces is extremely important for fluid wetting, hydration and clay

swelling and molecular sorption processes. It is commonly understood that this surface is inherently hydrophobic unless metal substitutions at Si or Al sites confer a net layer charge [3, 60]. However, the links between charge, water affinity and macroscopic wetting phenomena are subtle. For example, Rotenberg *et al*. (2011) showed that talc surfaces are highly hydrophilic with respect to the first molecular layer of water and that only when further water is added does it form non-wetting beads [61]. There is evidence from XRD determinations of water density profiles in 2:1 clays that increasing the layer charge alters the electronegativity of basal surface oxygens, thereby altering the affinity of water to that surface [62, 63].

Expandable clay minerals can incorporate water in their interlayer, thereby swelling or completely exfoliating as a function of water activity and ionic strength [64]. Clay swelling is challenging to describe quantitatively even in bulk solution because it depends on a balance of short- and long-range forces (including hydrogen bonding, electrostatic and van der Waals forces). Swelling and mobilization of clays into fractures dramatically reduces permeability for fluid flow [65] but the consequence of swelling for diffusive transport in clay rock is not clearly known and is typically neglected in simulations of diffusive transport [66].

Carbonates

Carbonate minerals play many important roles in clay rock. Calcite typically constitutes a large part of the fine-grained matrix along with clay minerals, but also occurs as elongated 50–100 µm-sized grains. Dolomite, siderite and ankerite occur, respectively, as core and rims of grains in most of the COx formation. The precipitation of carbonates in pores and fractures is a common cementation process in all clay rocks that can completely close advection pathways. Some clay rock contain abundant fibrous veins of calcite (occasionally gypsum or quartz) colloquially known as *beef* due to the resemblance with a fat-marbled steak. These veins are interpreted as representing natural hydraulic fractures within the shale due to fluid overpressure that were subsequently mineralized [67]. Moreover, calcite exerts a strong influence on pore water chemistry. Measurements of pH value and the dissolved carbonate concentration in the pore water of many clay rocks are suggest the aqueous solution is in equilibrium with carbonate mineral. [68] Carbonates also provide reactive surfaces for sorption and incorporation of solutes [69] (see below).

Other silicate minerals

Silicates, particularly quartz and feldspar, represent one of the three main mineralogical phases (Fig. 1) and may represent a large volume of the clay rock. It is an important structural component in shale characterized by low clay contents. However due to their low surface area and low dissolution rates at circumneutral pH, the impact of micron scale and larger scale silicates on ion diffusion is likely to be negligible. Some freshwater sedimentary rocks, including diatomite oil and gas formations in the US and the Horonobe RWS site (Japan), high-surface-area amorphous or crystalline silicates derived from the diatom biominerals are abundant [50]. Opals may present reactive surface areas, especially at high pH values.

Iron minerals

The high organic matter content of the sedimentary deposits that become shale rock readily lead to the development of reducing conditions. Consequently, iron is present in the reduced state except in weathered shales. For example, in the COx, iron was found by Mössbauer spectroscopy to be mostly (93%) present as Fe(II) and to be distributed over a wide range of mineral phases, such as pyrite, sideroplesite/ankerite and clay minerals. Iron(III), if present, was associated with clay minerals (probably illite, illite-smectite mixed layer minerals and chlorite) [70] or goethite nanoparticles [71].

Insoluble organic matter in clay rock

Clay rocks generally contain kerogen as dominant organic fraction, a fossilized macromolecular insoluble form of organic matter (OM) derived from biomass [72]. In studies of COx only 1.2% of the total organic carbon is extractable, most being present as insoluble (except in alkali and oxic conditions) kerogen organic matter [73]. The characteristics of insoluble OM vary widely depending on the source of the sediment (*e.g.*, continental or marine), the depositional environment (*e.g*. redox conditions and deposition rate) and the maturation degree which is dependent on temperature, pressure and time [48]. High deposition rates and reducing conditions favor high loads of preserved primary OM whereas low deposition rates and oxidizing environments enhance microbial degradation and loss of OM by oxidation. Certain gas shales including Woodford and Barnett contain abundant fecal pellets in the sub-mm size range. Fecal pellets are a form of OM with distinctive composition, including high phosphorus content, and

porosity [74].

Thermal maturation of OM following burial involves loss of oxygenated compounds, generating bituminous hydrophobic high-molecular-weight compounds. With increasing temperature (80-120 °C) residual OM starts to lose H and C atoms through thermal cracking reactions. The resulting products consist of both small polar compounds (organic acids, resins, asphaltens) and high molecular weight hydrocarbons. At higher temperature (generally above 120 °C) cracking of kerogen compounds leads to methane formation and a highly aromatic organic residue and sometimes graphite [75]. Sediments with immature and high amounts of terrestrially-derived OM display high O/C and H/C ratios, whereas mature OM having undergone methanogenesis shows the opposite.

Soluble organic matter in clay rock

The porewater chemistry of clay rock is very challenging to measure. Approaches include the equilibration of crushed rock with synthetic pore water (SPW) [76, 77], permeation experiments in which SPW percolates, under high pressure, through an intact clayrock core [77], and high-pressure squeezing methods [78]. All approaches should be performed anaerobically in order to limit changes in dissolved inorganic and organic species.

Pore waters from clay rocks in Belgium, France and Switzerland foreseen for radioactive waste disposal have been extensively analyzed. They show immature OM with variable amounts of organic matter and O/C ratios. The OM in Boom Clay, Belgium, exposed to a maximum burial temperature of 20°C, is the most immature with the highest O/C ratio, the highest TOC (1-5 wt%) and the highest dissolved organic carbon (DOC) in pore water (40-250 mg C/L) [79]. The COx and the Opalinus Clay formation (Switzerland) formations are fairly similar with regard to their OM characteristics, displaying a TOC content of up to 1 wt% and a DOC in the range of a few mg C/L [49, 76, 80]. The DOC predominantly contains low molecular weight (< 1000 Da) molecules such as mono- and di- acids with M_w < 350 Da (acetate, phenol, and propionic, tiglic, sorbic, suberic and lactic acids), amino acids, aldehydes, fatty and fulvic acids in smaller quantities.

Because DOC contains mostly anionic functional groups, transport through clay rock follows a similar pattern as inorganic anions, including the phenomenon of anion exclusion described

further below [81]. In surface and ground waters, DOC can enhance the transport of transition metals, actinides, lanthanides by means of complexes or colloid-facilitated transport. DOC from Boom Clay can transiently bind to and mobilize contaminants such as americium [82, 83]. DOC concentrations in COx and Opalinus clay rock are lower but can also enhance the solubility of trivalent lanthanides and actinides [84, 85].

2.2 Mechanical properties

All rocks can fracture under the application of stress or an increase of saturating fluid pressure [86]. At the Geological Carbon Storage site at In Salah, Algeria, geophysical monitoring suggested that the overpressure caused by CO_2 injection caused hydraulic fracturing of both the sandstone reservoir and the lower cap rock unit [24]. The analysis indicated that CO_2 migrated vertically into the lower cap rock through new and reopened fractures but did not compromise the upper mudstone cap rock. The geomechanical behavior of clay rock is evidently a vital consideration for the use of any formation as a seal and other applications. Although a full treatment of rock mechanics is outside the scope of this review, two aspects deserve highlighting.

Mechanical properties vs. *clay content*

The mechanical properties of clay rock vary considerably with composition, particularly clay content, which ranges from 10 to 65 weight % [9]. A critical threshold in clay mineral mass fraction, X_{clay}=0.34, separates fine-grained rocks with very different properties [87]. More brittle formations with a lower X_{clay} are currently the target of shale gas exploration because they are easier to fracture and to keep propped open. More ductile formations with higher X_{clay} have a higher tendency to self-sealing of fractures and thus more suitable as cap rocks for gas storage or repositories for nuclear waste. The conceptual model of Figure 2 explains this trend.

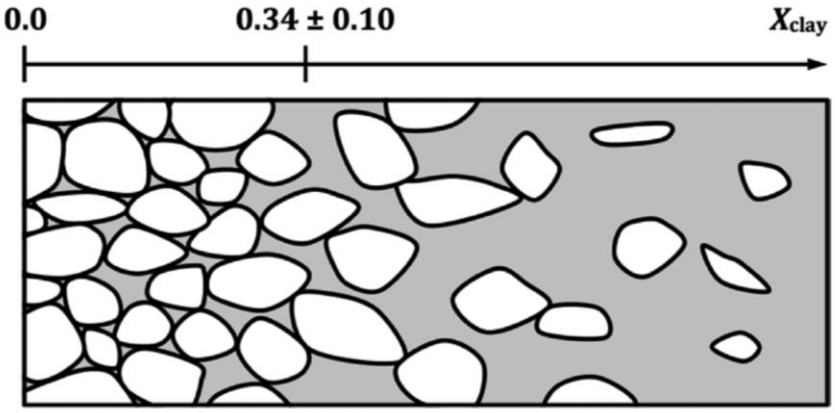

Figure 2. *A conceptual model of clay rock microstructure as a mixture of large grains (white) and a fine-grained clay matrix (gray) (Figure from [87] and [88])*

Porosity and transport under compression

The porosity of clay rock (described below) typically decreases exponentially with applied stress [89, 90]. As a consequence, laboratory studies of micropore and microfracture structure and transport conducted under ambient conditions may be inaccurate for the same rock in the subsurface. Moreover, microfractures observed in drilled core samples extracted from boreholes may occur during pressure relief (decompaction) and do not exist at depth. To date, relatively few studies of clay rock structure and transport were performed under relevant isotropic or anisotropic confining pressure [91, 92].

2.3 Structure

Clay rocks exhibit complex structure from the molecular scale to the basin scale. For example, the Marcellus shale consists of at least 6 lithofacies distinguishable by a suite of parameters [93]. Consequently, the macroscopic diffusion properties of clay rocks can only be understood by a multiscale knowledge of all structures and their spatial organization [94]. Clay rock communities are still grappling with the considerable challenges of determining, visualizing, and understanding the distributions of reactive surfaces, pores, minerals, OM and fractures to develop improve models of the transport, geochemical and mechanical properties of clay rock.

Mineral distributions

The distribution of mineral phases at the micrometer to millimeter scale has been performed

using two- and three-dimensional imaging techniques including scanning electron microscopy (SEM) and X-ray computed tomography with micron-scale resolution (µXCT). µXCT using laboratory or synchrotron sources can attain spatial resolutions below 100 nm in ideal cases, depending upon sample dimensions. The porosity measured by µXCT is therefore a small fraction of the total porosity, but this approach illuminates compositional and structural heterogeneity up to the critical centimeter length scale (Figure 3). For example, sedimentary rocks can retain signatures of biological activity following deposition. Burrows made by Cambrian worm-like organisms can be preserved in shale and completely filled with pyrite [94, 95]. Pyrite oxidation can subsequent generate preferential fluid transport paths. Because electron density contrast in SEM and µXCT is typically not adequate to unequivocally identify mineral phases, a combination of elemental composition information from 2D energy dispersive X-ray (EDX) fluorescence mapping at the SEM and 3D µXCT is becoming a popular approach.

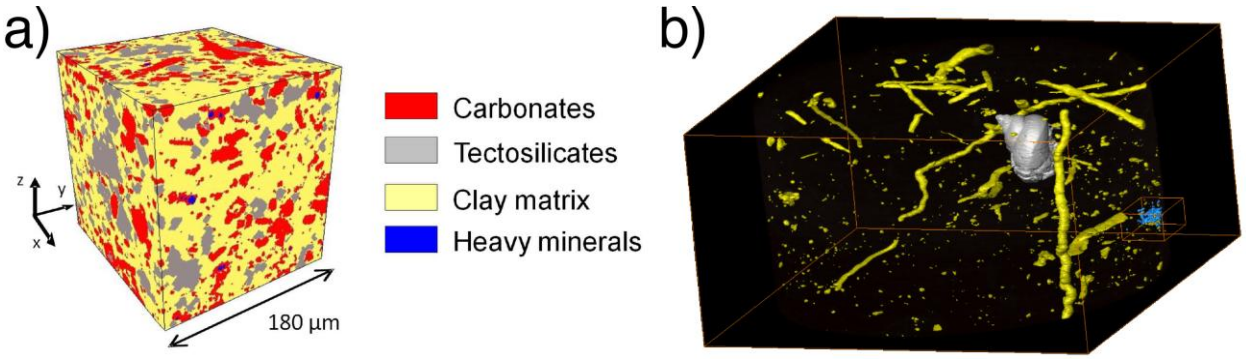

***Figure 3**: **a)** Mineral identification and distribution in the Callovo-Oxfordien (COx) using X-ray microtomography. Data from [94] **b)** Pyritized earthworm burrows in the COx. The dimensions of the parallelogram are 90 x 15 x 15 mm (J.C. Robinet, personal communication).*

Porosity

The pore volume of clay rock is typically between 10–30% and is distributed among all mineral and organic phases and the interfaces between them. Pores are due to a diverse range of clay rock constituents and inclusions [74]. A major challenge for clay rock research is determining the nature of the pores, their size distributions and their connectivity over a sufficiently large length

scale, often called a *representative elementary volume* (REV). The helium pycnometer is the most accurate method for measuring porosity in the laboratory. Gas adsorption isotherms using N_2, CH_4, *etc*., and mercury intrusion measurements can also provide complementary measurements of pore size distributions and specific surface areas (see [96]).

Serial focused ion beam (FIB) sectioning and scanning electron microscopy (SEM) can provide detailed 3D depictions of shale mineralogy, pore morphology and pore connectivity with 10–20-nm resolution and maximum imaging dimensions currently reaching ~100 µm (Figure 4) [15, 97, 98]. Helium ion microscopy (HIM) has the potential for reduced imaging aberrations, a smaller sample interaction volume and higher depth of focus than SEM, although few HIM studies of shale have been reported [99]. Transmission electron microscopy can provide detailed structural depictions and elemental compositions of 100-nm thin sections [100] or 500-nm FIB pillars [97].

All imaging methods that require sample drying are unable to accurately determine the structure of swelling clays in the original clay rock because desiccation leads to interlayer collapse and alteration of mesoscale structure. Cryogenic sample preparation has revealed unprecedented images of expanded smectite in salt solution [101]. The application to hydrated clay rock could significantly increase our understanding of hydrated pore connectivity but will require further development of this technique.

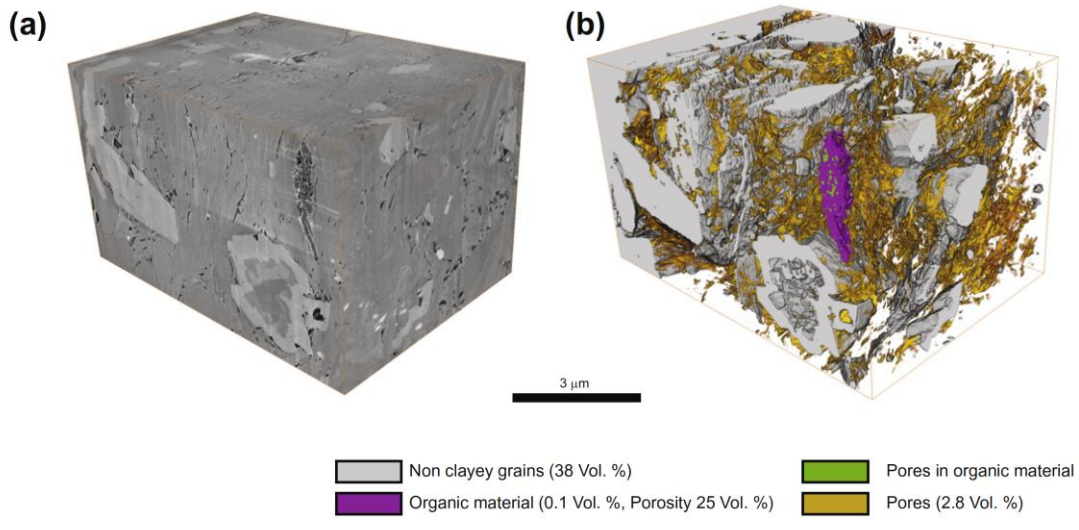

Figure 4*: Example of the determination of pore distribution in Opalinus clay using 3D FIB-SEM. a) Reconstruction of the analysed volume. b) Partitioning of the reconstruction into pore space and non-clay*

material. Data from [97]

Small-angle neutron scattering (SANS) can provide statistically relevant information on geometric pore sizes (Figure 5) [102]. SANS is superior to gas or Hg sorption studies in revealing true nanoscale porosity [99] although requires the addition of fluids, frequently isotopically labeled, in order to determine pore accessibility.

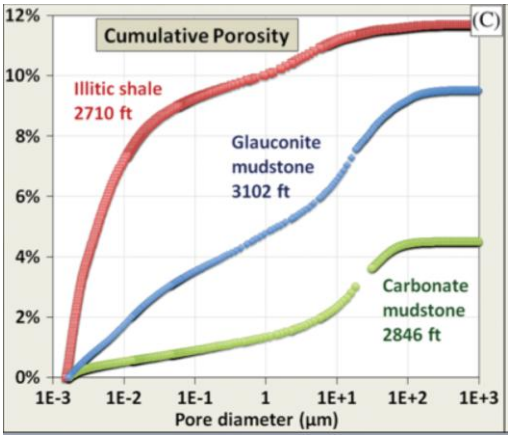

Figure 5*: Small-angle neutron scattering study of the porosity of different clay rocks. Figure from [102]*

No single imaging approach is currently capable of quantifying pores over a size range required to anticipate transport processes. For example, FIB-SEM of COx with a resolution of ~20 nm revealed only about 25-35% of the total porosity [97, 98]. Thus, experiments using multiple methods (particularly SANS and SEM or HIM) and that manipulate the fluids within clay rock are important. By combining FIB-SEM and TEM, Gaboreau *et al*. were able to visualize 70% of total porosity in a compacted illite analog of clay rock [103]. Using such an integrated approach, Gu *et al.* (2015) found that the dominant nanosized pores in a low organic, clay-rich shale samples were water-accessible sheet-like pores within clay aggregates [104]. The dominant nanoscale porosity in kerogen dominated organic-rich samples were found to be bubble-like organophilic pores [99, 104]. The porosity of shale organics is a strong function of thermal maturity with only mature organics exhibiting detectable porosity [105]. However, it remains unknown whether the bubble-like pores in shale organics detected by SANS or SEM are present under subsurface conditions or are generated when core samples are depressurized.

The chemistry and nanoscale porosity of the insoluble organic matter fraction of clay rock is quite inaccessible to conventional microchemical analysis. SEM imaging, for example, typically portrays the organic fraction as an undifferentiated gray scale level (*e.g.*, [106]). Scanning transmission X-ray spectromicroscopy (STXM) can use carbon K-edge absorption spectroscopy to identify kerogen thermal maturity and map carbon heterogeneity in organic-rich shales at 20-nm spatial resolution (Figure 6a) [100, 107]. Use of new coherent X-ray microscopy methods, including ptychography, will achieve higher spatial resolution than STXM and provide the full complex optical properties of a specimen, permitting phase contrast imaging that is more sensitive to low-density materials such as organics (Figure 6b). This method can also provide high-resolution 2D and 3D chemical and elemental mapping [108].

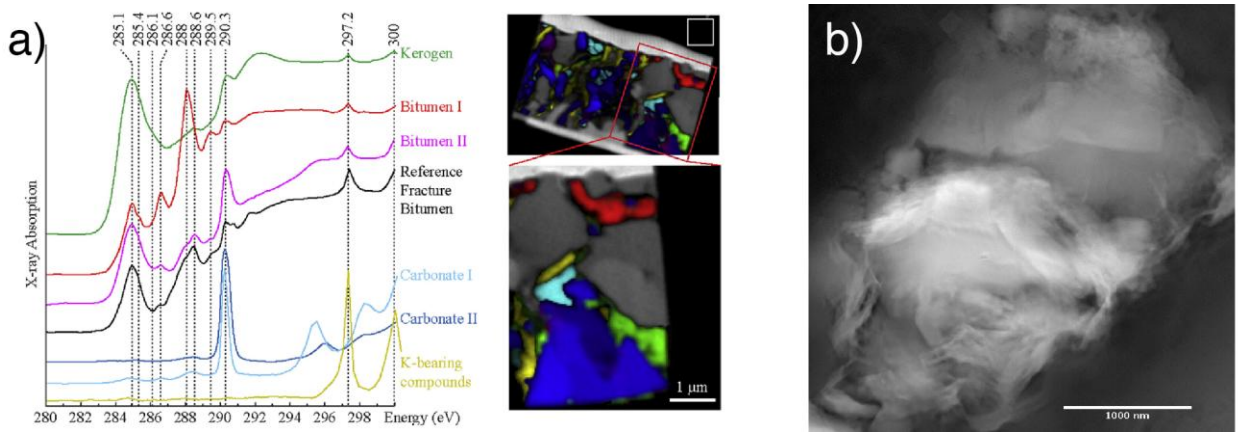

Figure 6. *Soft-X-ray microscopy studies of the organic components in clay rock. a) The organic components of an organic-rich mudstone can be distinguished using carbon K-edge X-ray absorption spectroscopy (left) and spatially mapped in FIB thin section using scanning transmission X-ray microscopy (right). Kerogen (green), bitumens (red and pink), carbonates (light and dark blue). Data form [100]. b) Coherent soft-X-ray microscopy image of an organic- and clay-rich fragment of Bakken shale. The phase image (shown) is sensitive to small differences in electron density within porous organics. Data from ALS beamline 5.3.2.1 courtesy of Namhey Lee, Peter Nico, Timothy Kneafsey, David Shapiro and Benjamin Gilbert.*

Pore Connectivity

There is growing evidence that the porosity detectable by most imaging studies is in fact poorly connected or unconnected at spatial scales larger than currently accessible [109]. For example, Keller et al. (2013) conclude that transport in Opalinus clay occurs predominantly through the nanoporous clay matrix [97]. King *et al*. (2015) noted that discrepancies in pore size distributions obtained by mercury intrusion porimetry and BIB-SEM imaging indicated that a major part of

the porosity was in fine pores not detectable by imaging [99]. Song *et al.* (2016) visualized connected pore networks in COx using 3D SEM and 2D TEM [98]. Pores of dimensions 50-90 nm formed percolating networks through the imaged volumes yet were likely unconnected at larger spatial scales. Thus, in many clay rocks, long-range transport must be constrained to occur through the finer porosity associated with organic- and clay-rich regions.

2.4 Permeability of Clay Rock

A quantitative measure of their sealing capacity is provided by the clay rock permeability, k (m^2), which is a property of the solid material affecting the dependence of fluid flow on the pressure difference. Low permeability (on the order of 10^{-20} m^2) is correlated with the low porosity of the clay rock as shown in Figure 7a [110] [110, 111]. Note that the permeability of clays is substantially larger than other minerals of the same porosity. This follows from the small size of clay particles and interstitial pore spaces and the affinity water to clay surfaces. The large variability in the porosity-permeability correlation displayed in Figure 7b is thus primarily related to the clay content [112]. For a given porosity, small differences in clay content may result in a dramatic change in permeability by several orders of magnitude. Factors such as stress history and the presence of natural or induced fractures also influence clay rock permeability.

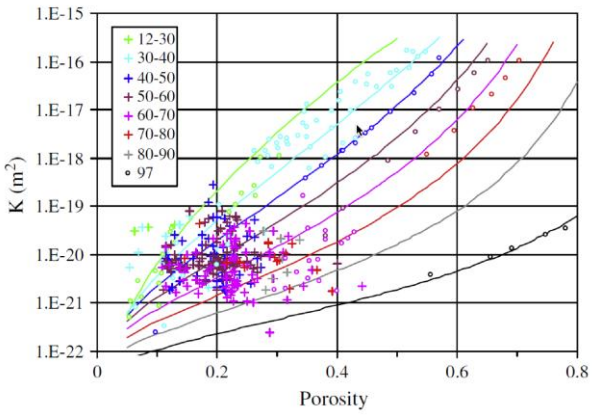

***Figure** 7: Trends in permeability (k) versus porosity shown for different clay contents ranging from 0–100% (shown in the inserted box) Data from [112].*

3. Diffusion in Clay Rock

Because of the very low permeability of non-fractured clay rock, fluid flow is not significant and diffusive transport mechanisms are dominant. Owing to slow transport rates, involving timescales that can extend into the thousands to millions of years, clay rocks are effective barriers for fluid flow and solute transport. There is abundant geologic evidence of the sealing capability of clay rock. For example, about one-half of the world's largest oilfields are sealed by clay rocks, the other half by evaporites [113]. Moreover, the profiles of ions from seawater traversing clay rock strata bounded by high permeability lithographies such as sandstone also provide clear evidence for the ultraslow transport rates (see Section 4).

3.1 Porosity–diffusivity relationships

Laboratory studies of solute diffusion through saturated clay rock or packed bentonite, combined with transport modelling (see below), can provide both effective diffusion coefficients and the accessible porosity for the mobile species. The exclusion of anions from pores formed between negatively charged basal surfaces, particularly the interlayer regions of smectites, is an extremely important influence on anion mobility. Anion accessible porosity can be less than half the total connected porosity of a clay-rich medium and even reduced to zero if mineral precipitation seals larger pores [114].

These studies also revealed a strong dependence of effective diffusivity on porosity. The relationship between effective diffusion coefficients (D_e) of a given species and porosity for a variety of formations has been described by an empirical relationship, termed Archie's law:

$$D_e = D_0 \phi^m \qquad (1)$$

where D_0 is the corresponding diffusion coefficient in water, ϕ is the porosity and m is the so-called cementation factor which is typically in the range of 2–3. This relationship has been analysed for a number of clay rocks [115, 116] as illustrated in Figure 8.

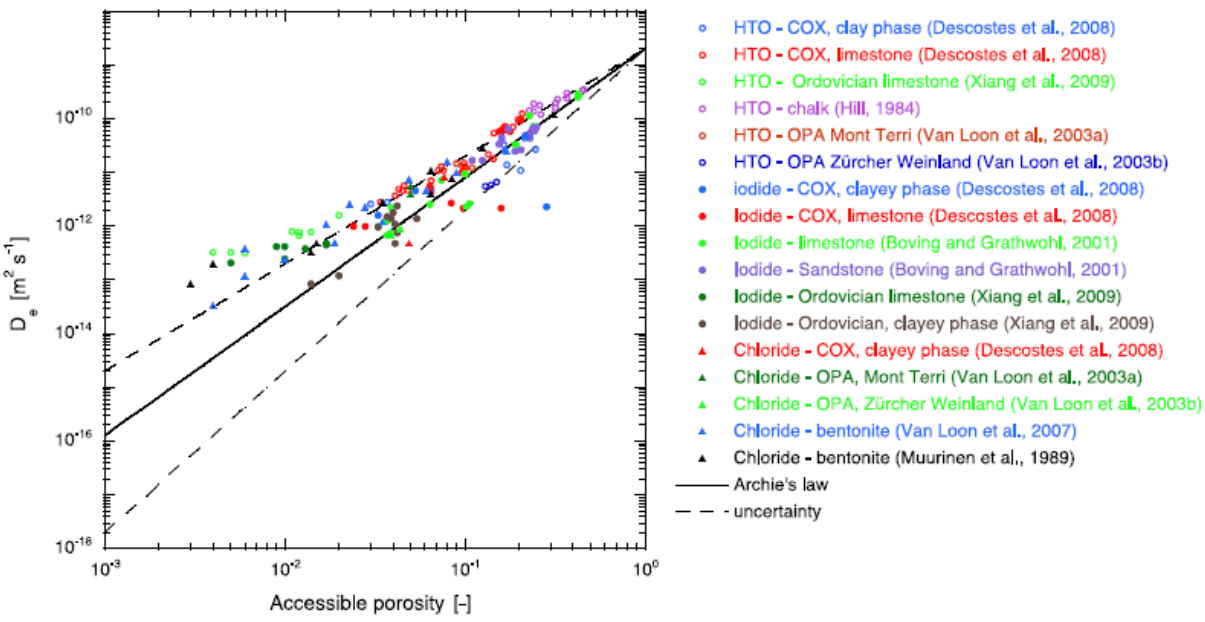

Figure 8. *Relationship between effective diffusion coefficient and diffusion-accessible porosity for tritium, chloride and iodide. The curves represent the (classical) Archie's relationship with m = 2.4 (solid line), m = 2 (upper dashed curve) and M = 3 (lower dashed curve). Figure from [116].*

3.2 Common factors controlling diffusive transport in clay rock

Driving forces for transport

Gradients in pressure, concentration and chemical potential lead to the flow of a fluid and the transport of solutes. In nanoporous media, the governing equations for transport frequently have an analogous form to Fickian diffusion, presented in more detail below.

Solubility

The solubility of mobile species in any fluid in the pore space of a clay rock is a major determinant of net fluxes. Meaningful predictions of the solubility of minerals and trace elements require expressions for ion activity products in H_2O–NaCl–$CaCO_3$–SO_4 systems under subsurface conditions. Solubility is well known for common substances but may be altered in nanoscale pores.

The solubility of a gas in a fluid is proportional to the partial pressure, as described by Henry's

law, and typically decreases with temperature and ionic strength but increases with pressure [117]. Molecules such as H_2 and CH_4 that do not react with water are much less soluble than molecules such as CO_2 that react with water when hydrolysis products are included. Thus, water-saturated clay rock could serve as a seal for $H_2(g)$ despite the high diffusivity of this molecule [33]. Many organic molecules can dissolve in and diffuse through supercritical CO_2, a process that enables enhanced recovery of oil [118].

Diffusion pathways

Net transport depends strongly on the nature, the volume and the geometry of transport pathways that are available in a clay rock, which can provide different pathways for ions, non-volatile molecules and gases. In any porous rock that is partially or fully saturated with brine, the transport of ions and dissolved soluble organic molecule occurs in the aqueous phase. In clay-rich regions, transport is constrained to occur through nanopores and interlayers. The different pathways of anions and cations in these regions lead to different effective diffusion rates [119, 120]. In low water activity systems, such as shale gas reservoirs, gases may flow through hydrophobic pore space or diffuse through pores saturated with any other fluid in which they are soluble.

For large systems, explicit (pore scale) descriptions of diffusion pathways are unfeasible. A simple upscaling approach is to define average properties of the porous medium, including porosity, permeability and geometric factors describing the transport pathways. Each species is then described by an effective diffusion coefficient. These upscaled parameters are typically inferred from macroscopic observations at the lab and field scale.

An important geometric parameter is the tortuosity factor, τ, that quantifies the travelled distance of a dissolved constituent through the pore network compared to actual distance between two points. Other factors such as narrowing and widening of pores or the pore connectivity are not inherent to this definition. Thus, a more general geometric factor can be used to describe the lumped effect of the geometry of the pore network on solute transport. For a clay rock sample, determination of ϕ and τ can be made through either bulk transport measurements or by direct imaging, but it is challenging to connect these measurements unambiguously.

3.3 Theoretical descriptions and conceptual models of the diffusion of solutes in clay rock

Diffusion of neutral and charged species

Diffusion of a solute due to a concentration gradient can be expressed in terms of Fick's first law which relates the diffusive flux of a species i to an effective diffusion coefficient $D_{e,i}$ and its concentration gradient in the x-direction according to

$$J_i = -D_{e,i}\frac{\partial C_i}{\partial x} \quad (2)$$

Fick's second law can be derived from equation 2 and the mass conservation in the absence of chemical reactions and describes the rate at which the concentration changes at any given point

$$\frac{\partial \phi C_i}{\partial t} = -\frac{\partial}{\partial x}\left(D_{e,i}\frac{\partial C_i}{\partial x}\right) \quad (3)$$

The effective diffusion coefficient $D_{e,i}$ is dependent on the porosity ϕ and the tortuosity τ of the porous medium according to

$$D_{e,i} = \phi D_{p,i} = \phi\tau D_{0,i} \quad (4)$$

where $D_{p,i}$ is the pore diffusion coefficient and $D_{0,i}$ the diffusion coefficient in water.

Fick's law does not consider the electrostatic interaction between ions and it is therefore strictly valid only for uncharged species. If diffusion of charged species is considered then electrochemical migration needs to be included in the flux term such that positively and negatively charged species move in a coordinated manner to maintain local charge balance. The combination of molecular diffusion and electromigration can be expressed by the Nernst-Planck equation that considers diffusive transport of all species including charged species under the influence of an electrical potential (*e.g.* [59]). The corresponding flux is

$$J_i = -D_i\nabla C_i - \frac{D_i C_i}{RT} z_i F \nabla\varphi \quad (5)$$

where z_i is the charge of species i, F and R are the Faraday and gas constants, respectively, T is the temperature and φ is the electrical potential. Other coupled transport processes may be significant at long timescales. For example, a thermal gradient developed in a nuclear waste repository can establish a gradient in osmotic potential and net mass transport [121, 122].

Ion diffusion in the vicinity of charged mineral surfaces

Clays (and other minerals) in water often develop a negative surface charge giving rise to an electrical field that attracts cations and repels anions. The diffuse layer of excess cations and depleted anions is known as the electrical double layer (EDL) [64]. Further away from the mineral surface, where the electrical potential becomes weaker, the pore water becomes internally charge balanced. Within clay rock, the dimensions of pores and clay interlayers can be similar to the size of the EDL. Consequently, anions may be partially or totally excluded from a fraction of the pores and interlayers. This effect increases with increasing compaction of the clay and alters the diffusion paths and effective diffusivity of anions relative to cations and neutral species [111, 119]. The concept of anion accessible porosity and the effect of anion exclusion has been observed in many experiments carried out on clay materials [7].

The negative structural charge on some clays may not completely exclude anions from interlayers. For example, recent MD simulations (**Figure 9**) suggest that electrostatic effects may only partially exclude anions from smectite interlayers [123]. Moreover, anions may enter the interlayer as part of a contact ion pair, particularly when the partner cation has a higher charge. This has been shown macroscopically in the case of ions pairs formed between Cl^- and Ca^{2+}, Mg^{2+} and Fe^{2+} [124, 125], by XRD [126], Mössbauer [124] for $FeCl^+$ and $CaCl^+$ [124]. No data exist today, to our knowledge, on the adsorption of $CaCO_3°$, $MgCO_3°$ or $CaHCO_3^+$ ion pairs, although these ion pairs are now proposed to be important precursors for the formation of amorphous calcium carbonate (ACC) and magnesium analogs [127].

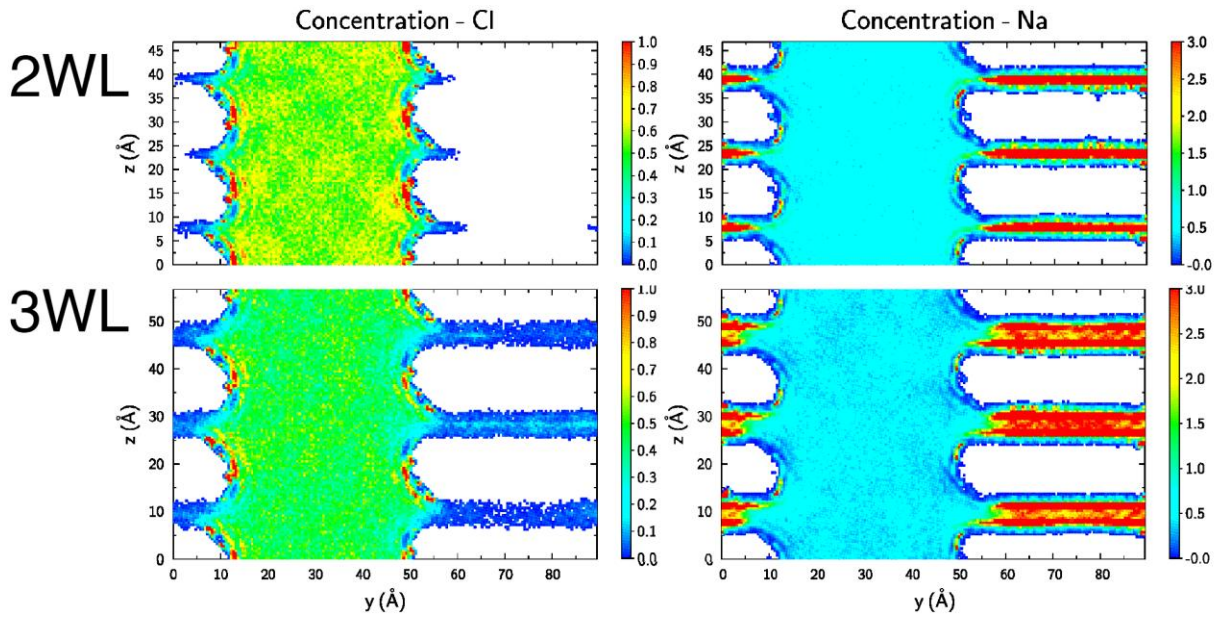

Figure 9. *Molecular dynamics simulations of cation incorporation and partial anion exclusion from the interlayer regions of montmorillonite. The white zones are the smectite layers and the coloured regions depict the concentration of* Na^+ *and* Cl^- *time-averaged for up to 50 ns. This work shows that anions such as* Cl^- *are excluded from the two-water-layer (2WL) crystalline hydrate of montmorillonite but partially enter the 3WL hydrate. Figure modified from* [128].

Linking molecular dynamics and macroscopic transport in nanopores

The dynamics and transport of solutes within spatially confined environments close to electrostatically charged mineral surfaces is a subject of intense study. In these settings some fundamental properties of water (structure, viscosity, dielectric constant and self-diffusion dynamics) are different from bulk values. Experimental and simulation studies typically address a single timescale from picoseconds (*ab initio* simulation and quasi-elastic neutron scattering, QENS); nanoseconds (classical simulation, *e.g.,* Figure 9); microseconds (nuclear magnetic resonance and dielectric relaxation spectroscopy). Integrating the information obtained from these complementary approaches to determine a complete model of water structure and dynamics continues to be a challenging endeavor. Sposito and Prost (1982) showed the interlayer water structure to be dependent on the time-scale probed by the various spectroscopic studies used [1]. Sanchez *et al*. (2009) found activation energies for water diffusion in compacted montmorillonite to be different when derived by macroscopic diffusion or QENS [129]. Diffusion of water within

smectite interlayers is retarded by surprisingly long-range electrostatic interactions that can extend across the 2:1 layer [130].

Good progress has been made in reconciling the micro- and macro-scale diffusivity of ions. Tertre *et al*. (2015) obtained good agreement in predicting the diffusion of Ca^{2+} through the interlayer of vermiculite single crystals that entirely lacked any tortuosity [131]. Tinnacher *et al*. (2015) showed that macroscopic transport of cations, anions and neutral molecules can in packed clay can be well predicted from molecular simulation [132]. Gimmi and Kosakowski (2011) compiled a large set of diffusion coefficients for various cations in clay and used these to derive a simple surface diffusion model which is based on an average surface mobility that relates the mobility of surface cations to their diffusion in bulk water. The interpretations of all studies in dense clays systems are ambiguous, however, without better constraints on nanoscale pathway connectivity.

Colloid transport

In saturated rock, transport of poorly soluble species may occur via colloid transport. Indeed, because of the reducing environment of most clay rocks, the dissolved concentration of radionuclides is limited by the low solubility of their reduced form. However, natural organic matter in Boom Clay can bind amorphous UO_2 nanoparticles forming uranium containing colloids ranging in size from 2–450 nm at concentrations 3 orders of magnitude higher than the solubility of the precipitate. Nevertheless, colloid mobility in unfractured clay rock is very low and U(IV) migration does not appear to be enhanced by the formation of inorganic-organic colloids. [79, 133]. A study of Opalinus clay also concluded colloid transport to be negligible [134].

3.4 Theoretical description and conceptual models of the transport of gases in clay rock

Gas transport through low-permeability rock formations is controlled by gas pressure, the hydraulic and mechanical properties of the rock (*i.e.*, intrinsic permeability, porosity, and rock strength), the hydromechanical state of the rock (*i.e.*, water saturation, pore water pressure, and

the stress state of the rock) [135]. Gas interactions with rocks and fluids can lead to dynamic changes in flow regime depending on gas pressure (Figure 10) [12, 136].

Gas transport regimes

When the gas pressure is below the pore water pressure, gas remains dissolved in the aqueous phase and is transported by Fickian diffusion due to concentration gradients. The water phase itself may flow as a consequence of hydraulic pressure gradients, although this process is not likely to be significant in tight clay formations.

If the gas pressure exceeds the pore pressure, gas will exsolve from aqueous solution forming a separate fluid phase. This phase will displace water from the pore network if the gas pressure exceeds pore entry pressures (also called capillary threshold pressures) that are inversely correlated with the pore radius. Water tends to be replaced in large pores first and more pathways for the gas will form at higher pressure as increasingly narrower pores are drained. If the gas phase forms a connected network then pressure-driven transport will occur at a rate that is determined by the permeability of the accessible rock. A mathematical description of gas transport in this regime is given below.

If the gas pressure exceeds the minimum principal stress acting on the rock, micro-fracturing or dilation of the rock will occur which in turn increases the porosity and intrinsic permeability. If the gas pressure exceeds the sum of the minimum principal stress and the tensile strength of the rock, macroscopic tensile fractures may form. These fractures may constitute preferential fluid pathways enabling flow rates orders of magnitude higher than in the bulk rock. This process is a failure mechanism of serious concern for geological carbon sequestration. However, fracture propagation ceases when the gas pressure in the fractures becomes less than the value of the minimum principal stress [135].

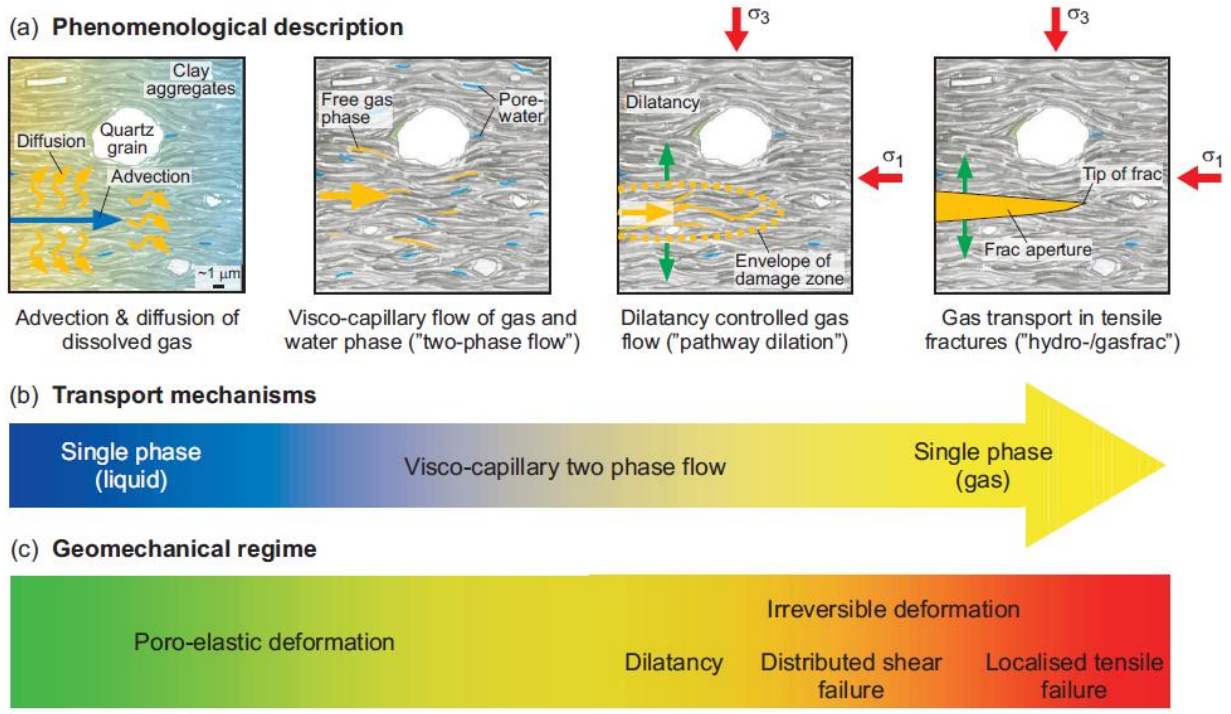

Figure 10: Classification and analysis of gas transport processes in the Opalinus Clay, Switzerland after [135]. Panel a) Phenomenological description of the different regimes of gas transport 1) fully saturated with aqueous phase, 2) 2-phase conditions and 3) fully saturated with gas phase. Panels b) and c) show the basic transport mechanisms and the geomechanical regime, respectively.

Mathematical models of gas transport

Gas transport through a porous medium can be described by several models depending on the pore length scale, r, and the mean free path, λ, of gas molecules between collisions. The Knudson number, $K=\lambda/r$, is a dimensionless parameter commonly used to classify flow regimes in small pores where deviation from continuum behavior is important.

When pore dimensions are large ($K<0.01$), pressure-driven fluid transport at the pore scale is described by the Navier-Stokes equation. This statement of the conservation of momentum for a compressible, viscous fluid, combined with the continuity equation for the conservation of mass and explicit pore wall boundary conditions, yields an explicit flow field for a given pressure difference. Flow through complex geometries such as a fracture in a shale can be predicted using numerical simulation but requires high-performance computing and efficient algorithms [137].

A simplified, upscaled description of net fluid flow through a porous medium is provided by Darcy's law. The flux in fluid density in 1D for a fluid of viscosity μ subjected to a gradient in pressure, P, is given by

$$J_D = -\frac{\kappa}{\mu}\frac{\partial P}{\partial x} \quad (6)$$

The Darcy permeability, κ (m^2), is a constant of proportionality determined by experimental measurements of gas flow as a function of pressure difference. The mass balance equation then has a similar form to Fick's second law:

$$\phi\frac{\partial \rho}{\partial t} = -\frac{\partial}{\partial x}\left(\frac{\rho\kappa}{\mu}\frac{\delta P}{\delta x}\right) \quad (7)$$

This expression neglects gas sorption processes that are important for gas transport through clay rock. Darcy's law has been used successfully for liquid and gas flow in reservoir rocks with pore dimensions down to about 1 μm.

At smaller pore dimensions ($0.1<K<10$), the flow of a gas is higher than predicted. Beginning with Klinkenberg, several corrections to Darcy's law have been proposed based on the concept that the no-flow condition for liquids at an interface do not hold for gases [138]. When pore dimensions approach the molecular scale ($K>10$), continuum descriptions cannot be applied and gas flow in this regime has been described as purely diffusional with negligible viscous effects [139]. Cui *et al*. (2009) summarize experimental methods for determining rates of diffusive gas transport in clay rock [140]. Jacops et al. (2015) and Marschall *et al*. (2005) give examples for different clay rocks [141, 142].

4. Diffusion through clay rock formations

The rates of solute transport through clay rocks on a formation scale can be assessed by measuring and interpreting concentration profiles of natural tracers such as halogens (Cl^-, Br^-, I^-) and their stable isotopes (^{37}Cl), water isotopes (^{18}O, ^{2}H) and noble gases (He, $^{3}He/^{4}He$, Ar, $^{40}Ar/^{36}Ar$). Concentration profiles of natural tracers are controlled by the conditions under which the clay rock was deposited and by the hydrogeological evolution of over- and underlying strata that can lead to diffusive exchange of tracers between the strata and the clay formation.

Numerical models can be used to integrate the conditions upon clay deposition, transport properties of the clay and the paleo-hydrogeology and simulate the evolution of a site by matching observed and simulated tracer profiles. In these simulations, the conditions upon clay deposition and the hydrogeological evolution define the initial and boundary conditions of the model, respectively. Note that a well constrained, integrated assessment of evolving tracer concentration profiles in clay formations is possible only if the diffusion of tracers is in a transient state. If diffusive transport has attained steady state or has ceased altogether, it is no longer possible to constrain the time at which the hydrogeological perturbation of conditions in the over- and/or underlying strata occurred and thus to place the evolution of the system into a paleo-hydrogeological context. This implies that the timeframe over which this kind of integrated analysis can be carried out is typically limited to a few millions of years into the past.

4.1 Interpreting chloride profiles at selected sites

Here we present natural Cl^- profiles from selected sites and interpret them in the context of the hydrogeological evolution of that site. The clay rock formations described below were all deposited in marine environments with an initial pore water composition of seawater assumed to be equal to the current conditions of $Cl^- = 546$ mmol/kg_w for an average salt content of 35 g/L. Changing depositional environments led to the formation of more permeable rocks such as carbonate rocks or sandstones above and below the clay formation. Over geological times, tectonic activity caused uplifting, deformation and erosion thus altering the hydrogeological conditions. Permeable rocks became exposed at the surface and subject to freshwater recharge and thus turned into freshwater aquifers. These changes in the hydraulic regime and the ensuing change to low-salinity conditions in the permeable rocks initiated diffusive exchange with the saline porewater in the clay formation sandwiched between the aquifers. Current profiles of anions (and other natural tracers) in clay formations are a reflection of the diffusive transport history that began with the recharge of dilute groundwater into the over- and/or underlying aquifer (Figure 11).

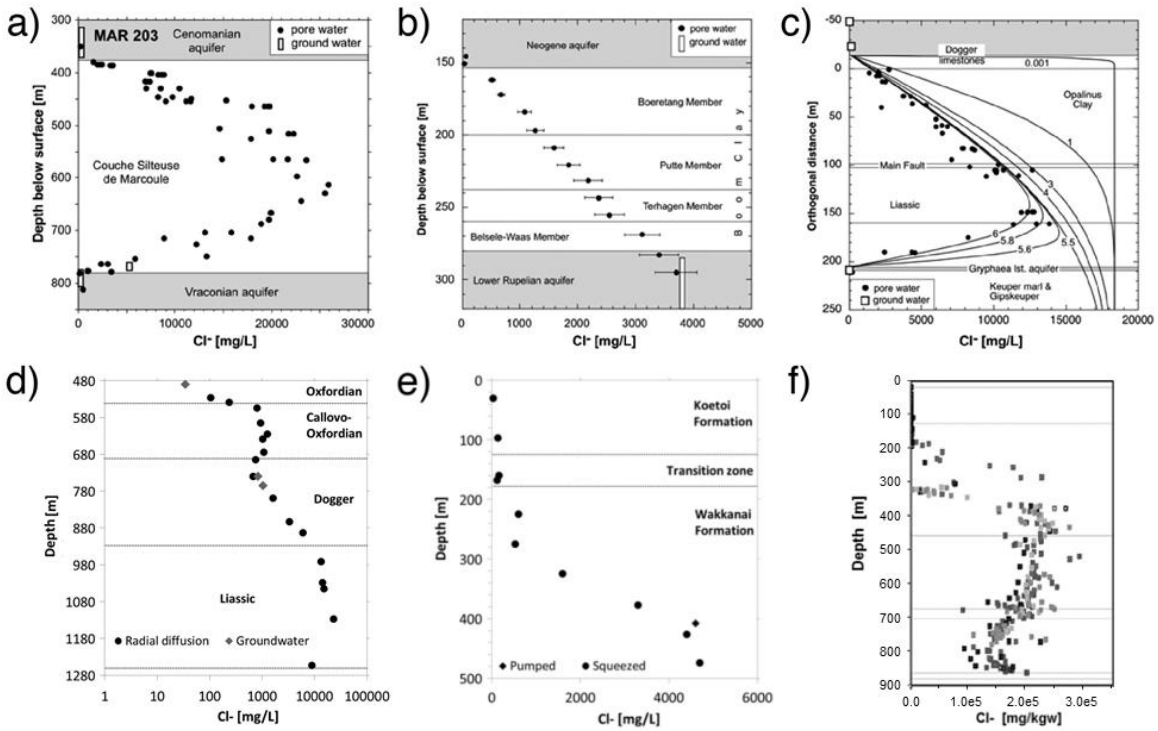

Figure 11. *Chloride profiles through selected clay rock formations.* ***a)*** *The Couche Silteuse at Marcule (France) shows a symmetric profile of Cl^- concentrations with a concentration maximum at mid-depth indicating the simultaneous freshwater recharge into the over- and underlying aquifers and ongoing outdiffusion of Cl^- into these aquifers.* ***b)*** *The linear Cl- profile through the Boom Clay at Essen (Belgium) shows that steady state conditions have been attained.* ***c)*** *The Opalinus Clay at Mt. Terri shows an asymmetric Cl^- profile with a concentration maximum shifted towards the bottom aquifer, indicating a late activation of the bottom aquifer. Shown are also results from a modeling study that almost perfectly match the measured profile. Data in a-c are from [111, 120].* ***d)*** *Chloride profile through the Callovo-Oxfordian (COx) formation, Bure (France). Slower Cl^- than deuterium diffusion into the overlying aquifer is a consequence of anion exclusion. Data from [143].* ***e)*** *Chloride profile through the Koetoi and Wakkanai mudstones at Horonobe (Japan). Data are from pumped water and squeezed groundwater samples. Data from [50, 144].* ***f)*** *Chloride profile (in mg/kgw) from the Cobourg formation, Ontario (Canada). Data from [9]*

Couche Silteuse, Marcoule (France)

The Couche Silteuse at Marcoule in France is a Cretaceous marine silty-shaly formation of variable thickness and depth (163–404 m and 377–1066 m. It is situated between two sandstone aquifers [145]. The Couche Silteuse was deposited in the Mediterranean Sea and Cl^-

concentrations in the pore water may exceed those of present-day seawater due to the proximity of evaporites. The symmetric Cl^- profiles observed at the thickest locations of the shale layer (Figure 11a) are a consequence of anion diffusion into the low-salinity Na-HCO_3^--dominated groundwater in the aquifers above and below the formation that are continually recharged by freshwater [111, 120].

Boom Clay, Mol and Essen (Belgium)

The Boom Clay formation at Mol (103 m thick) and at Essen (127 m) is a clay unit deposited in a marine environment in the Rupelian stage of the Oligocene (33.9–28.1 Ma), bounded above and below by sandy aquifers. The overlying Neogene aquifer is continually recharged by freshwater aquifer while the underlying Lower Rupelian aquifer has retained ~20% seawater salinity. The Cl^- profile at Essen shows a linear diffusion profile between the two aquifers, demonstrating that out-diffusion has erased the marine signature of the initial Boom Clay pore water and a steady-state diffusion regime has been reached (Figure 11b) [111, 120].

Opalinus Clay, Mt Terri (Switzerland)

Mt. Terri is an anticline in the Folded Jura Mountains in NW Switzerland [146]. The Opalinus Clay at Mt. Terri is a 219-m thick, clay sequence deposited in a marine environment during the mid-Jurassic (180 Ma). It is overlain and underlain by permeable carbonate aquifers that became infiltrated by freshwater as a consequence of folding and subsequent erosion of the anticline. The Cl^- profile of the Opalinus Clay shows evidence of a diffusive flux into the aquifers (Figure 11c). In contrast to the symmetric profile in the Couche Silteuse, the profile at Mt. Terri is strongly skewed because the overlying Dogger aquifer has been exposed to freshwater recharge earlier than the underlying Lias aquifer. Figure 7c includes results from a numerical simulation that almost perfectly reproduces the Cl^- concentration profile in the Opalinus Clay. The simulation is based on assuming an initial concentration of 18.4 g/l following first freshwater recharge of the Dogger aquifer at 6 Ma and a subsequent recharge of the Lias aquifer at 0.5 Ma. The timing of the activation of the aquifers inferred from this model fits well in the overall geological history (*i.e.*, uplift and erosion) of that site derived from other geological evidence [111, 120].

Callovo-Oxfordian (COx) formation, Bure (France)

The 140 m thick Callovo-Oxfordian (COx) clay rock (160 Ma) contains 25-55% clay including illite/smectite mixed layers, illite, chlorite and kaolinite. The COx formation has been selected as the host formation for installation of a future underground radioactive waste disposal facility in France. The French National Radioactive Waste Management Agency (ANDRA) has built an underground research laboratory (URL) in Bure (NE France) in order to study the disposal of radioactive waste in a deep clay formation [147]. Profiles of stable isotopes and chloride through the COx show that this formation is highly out of equilibrium with the upper Oxfordian aquifer and the lower Dogger aquifer (Figure 11d). Modeling deuterium profiles suggested that groundwater out diffusion from COx into the upper and lower aquifers begun between 1.5-5 Ma, depending on the assumed initial concentration. In contrast, modeling Cl^- profiles assuming an anion accessible porosity of 50% of the total porosity yielded much longer diffusion times. These differences were attributed to spatial variations in the anion accessible porosity, uncertainties in the diffusion coefficient or uncertainties in the assumed initial Cl^- concentration [143, 148].

Horonobe Underground Research Laboratory (Japan)

The Japan Atomic Energy Agency (JAEA) has chosen a sedimentary host rock as a candidate for deep geologic disposal of nuclear waste and established an underground research laboratory at Horonobe. The Cl^- profile (Figure 11e) shows a distinct increase in the Cl^- concentration from the Koetoi into the underlying Wakkanai formation [144]. The sedimentary sequence was deposited in a marine environment during the formation of the Japan Sea (15 Ma-5 Ma). These deposits were intermittently inundated by pyroclastic flows which means that volcanic deposits occur intercalated within the sedimentary sequence. The Koetoi Formation is composed of diatomaceous soft mudstones, while the underlying Wakkanai formation shows a higher degree of diagenesis and contains cristobalitic porcelanite (Opal-CT). Biogenic opal in the diatomaceous sediments has dissolved and re-precipitated as cristobalite during the basin filling. The Koetoi formation has a maximum porosity of about 60% whereas the Wakkanai formation has porosities of 30-40%. Similarly, the hydraulic conductivity decreases with depth [149]. All these changes with depth are caused by a higher degree of diagenesis at greater depth [50, 149]. The Cl^- profile in Figure 11e is a reflection of decreasing diffusivity with increasing degree of diagenesis.

Deep Geologic Repository (DGR) at the Bruce nuclear site, Ontario (Canada)

The Bruce site is a proposed location for a deep geologic repository for low or intermediate level nuclear waste [9]. The site consists of 9 hydro-stratigraphic units with the very low permeability, Ordovician (450 Ma) Cobourg Formation located at 1675 m depth. The layer silicate fraction in this limestone is <10% and includes illite & micas, chlorite, illite/smectite with trace amounts of kaolinite. The natural tracer profiles, including the Cl^- profile (Figure 11f), were interpreted by a model in which diffusion into the Cobourg formation from hypersaline overlying Cambrian evaporites occurred for up to 250 million years. Recent infiltration of freshwater caused an abrupt concentration discontinuity that is only beginning to re-equilibrate.

4.2 Perspective on formation-scale simulations

The above examples show that it is possible to use concentration profiles of natural tracers in combination with the recent paleo-hydrogeological evolution of a site to constrain formation scale effective diffusivities in clay rocks. These studies clearly demonstrate that non-fractured clay rock is a barrier for the transport of inert solutes. Reservoir simulations can similarly achieve good quantitative prediction of methane production from tight shales. Typically, however, the effective transport rates used in such continuum models encompass a range of chemical processes in addition to diffusion. Many species of interest for clay rock systems are reactive in ways that can dramatically alter their mobility and these processes are addressed below.

5 Sorption and Reaction of Gaseous and Anionic Species in Clay Rock

Sorption or chemical interactions with mineral or organic phases can retard a diffusing ion or molecule and increase the storage capacity for that species within a clay rock. Here we survey key mechanisms and current knowledge on reaction processes of some important species in clay rock.

5.1 Retardation Mechanisms

Sorption and ion exchange

Clays and micas can retard cations through adsorption at edge sites and ion-exchange reactions with interlayer species [58, 150-153]. Anions including long-lived radioisotopes such as $^{36}Cl^-$ or

$^{129}I^-$ generally exhibit a much lower sorption affinity for clays and thus restriction of transport is more dependent upon geometric limitations (including transport limitation due to anion exclusion). As shown below, for some anions such as SeO_3^{2-}, retardation can also be driven by incorporation into carbonate minerals or chemical reaction, while for other such as I^- sorption is negligible.

Kerogen and clays can both exhibit high sorption capacities for gases including CH_4, CO_2 and H_2 (see below). These adsorption processes contribute to the capacity of clay rock for gaseous species and retard gas transport and it can be challenging to distinguish organic matter and clay contributions [142].

Descriptions of adsorption range from simple to complex geochemical models. Simple affinity coefficients, such as K_D values, are only valid for the measurement conditions but provide a method to estimate transport over long timescales. Gas adsorption to kerogen or to clay rock often described by semi-empirical functions such as the Langmuir isotherm that assumes monolayer sorption or Freundlich isotherms that assume a series of K log-normal distributed Langmuir isotherms [7]. Surface complexation modeling is the most versatile approach for mineral sorption reactions in which the stoichiometry and surface binding site(s) are well known [153].

Mineral reactions

Mineral precipitation and dissolution are basic processes that control water chemistry and porosity in rocks [114]. Rates of mineral dissolution are well known to be difficult to constrain by laboratory studies. Rates of mineral nucleation are even more challenging because the activation barriers for homogeneous and, especially, heterogeneous nucleation can be very sensitive to chemical conditions. Moreover, mineral precipitation in nanoscale pores may be influenced by surface interactions that can either suppress or enhance reaction rates [154].

5.2 Gases

$CO_2(g)$

Clay rock has a significant storage capacity for CO_2 that is due to dissolution in pore water as well as adsorption to clay minerals. For example, Busch *et al*. (2008) reported bulk averaged

CO_2 concentrations of Muderong shale exposed to $scCO_2$ (222–389 mol/m^3) that far exceeded concentrations attained in coal (3–4 mol/m^3) or cemented sandstone (8–10 mol/m^3) [155]. The high affinity of clays for CO_2, particularly the intercalation of CO_2 within smectite interlayers, was a surprising finding that has been replicated by many studies in recent years [156-158]. CO_2 uptake by smectite can additionally cause interlayer expansion depending on the initial hydration state of the clay, interlayer cation and the confining pressure [156]. While the extent of the measured clay swelling is relatively small (<3%) it could be sufficient to reduce the permeability of GCS caprock, thereby enhancing storage.

The above laboratory studies were performed on relatively short timescales. However, indefinite exposure of caprock to $scCO_2$ that is not saturated with H_2O could eventually dehydrate and collapse swelling clays, potentially leading to the formation of new advection pathways. Moreover, there is evidence that CO_2 is not an inert adsorbate but either $scCO_2$ or carbonated brines can react with the surfaces of silicate and clay minerals, altering interfacial properties. Wan *et al*. (2014) showed that exposure to $scCO_2$ alters the hydrophilicity of mica [159] and the morphology of mica surfaces (personal communication). Exposure of smectite to dry $scCO_2$ can lead to carbonate mineral precipitation [160] that could weaken caprock integrity [161].

CH_4 and volatile hydrocarbons

The sorption of methane by organic rich shale rock is likely dominated by kerogen, the insoluble organic matter component. Sorption correlates well with OM content [162] and the heats of adsorption are greater for organic matter than for clay minerals [163]. Nevertheless, clay minerals also contribute a high surface area for gas sorption, as clearly shown by a study in which the OM content was chemically removed by NaOCl [105]. Fundamental insight into gas interactions with kerogen is limited by a lack for the molecular and nanoscale structure of this complex and variable substance. Recently, Bousige *et al*. generated molecular models for kerogen of 3 different geologic origins that satisfied experimental constraints on carbon atom distributions, elasticity and porosity [164]. This opens a pathway for molecular studies of sorption and transport that have currently been confined to idealized mineral systems.

Methane sorption to smectite shows a strong dependence on surface charge, which modifies basal layer hydrophobicity, and pressure. Sorption isotherms follow a Langmuir profile with a

maximum monolayer sorption of 5.7 mol/kg reached at 30 MPa and above [165]. At low pressures, interlayer CH_4 molecules in Na montmorillonite are solvated by 12–13 waters, with 6 oxygen atoms from the clay surface completing the coordination shell (Figure 12) [166, 167]. At 1 MPa and 300K, a clathrate-cage structure develops around the methane molecule in the 3-layer hydrate smectite interlayer, with 0.5 CH_4 per clay unit cell [6]. Shale gas production may be causing an increase in ethane emission to the atmosphere and the storage and release capacity of methane containing shales is not well understood [19].

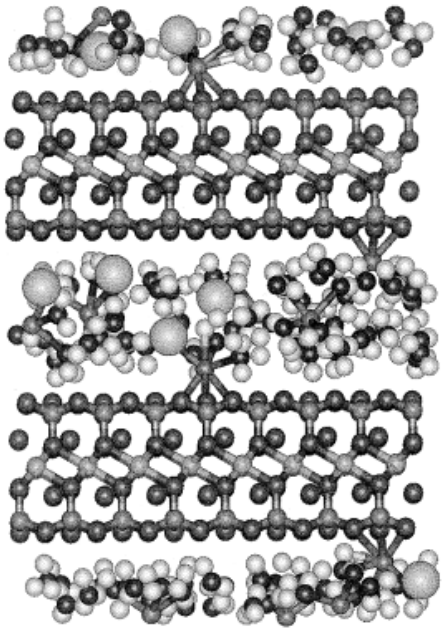

***Figure 12**. Snapshot from a molecular dynamics simulation of methane molecules within hydrated sodium montmorillonite at 340K and 300 bar, conditions equivalent to a burial depth of 2.0 km. CH_4 molecules are depicted as large gray spheres, Na^+ ions as small black spheres. Image from [166]*

$H_2(g)$

The interactions of hydrogen gas with clay rock have been principally investigated within the context of high-level radioactive waste storage. $H_2(g)$ is an anticipated product from the anoxic corrosion of stainless steel waste containers and from water radiolysis reactions caused by alpha decay [11]. If H_2 gas cannot escape from clay-rich media faster than it is generated, pressure build up could diminish the stability of the repository [142]. In addition, certain proposals for

geologic storage of H_2 generated by excess renewable energy also require clay rock to serve as an impermeable and inert cap rock for H_2. Detailed studies for relevant formations are currently lacking, however, in part because performing diffusion and sorption experiments with H_2(g) on natural clays and clay rock is difficult. Set-ups are prone to leakage [168] and microbial processes can interfere (transforming H_2 to CH_4) [142, 169].

Hydrogen sorption onto dry clay rock can reach ~0.1% in weight [170], a similar value to methane and CO_2 sorption onto clay-rich media [171] (Figure 13). However, water competes strongly with H_2(g) for adsorption on hydrophilic clay surfaces, and in water fully saturated conditions, H_2 diffusion measured in undisturbed Boom Clay and Cox cores showed no sorption effects *[171]*. Hydrogen sorption on clays with low water content is thus most relevant to nuclear waste repositories during the unsaturated period following the closure of the galleries.

Neutron scattering has revealed the structure and dynamics of molecular H_2 physisorbed in the interlayer space of montmorillonite and laponite [170, 172, 173]. Up to four hydrogen molecules coordinate directly to partially solvated interlayer Ca^{2+} cations. H_2 transport occurs via a jump diffusion mechanism leading to a H_2 diffusion coefficient an order of magnitude slower than in bulk liquid water [173].

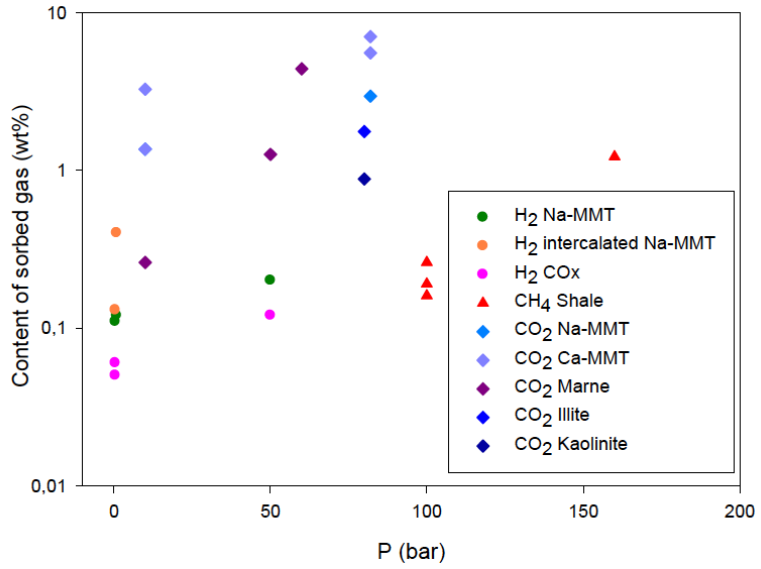

***Figure 13**. Adsorption isotherms of hydrogen, methane and carbon dioxide on clays and clay rock. MMT=montmorillonite. COx = Callovo-Oxfordian. Data from [171]*

Competitive gas sorption processes

Gas storage and transport processes in clay rock always involve competition among intrinsic and injected gases and water molecules for sorption sites. For example, field and laboratory studies have shown that CO_2 can displace methane from sorption sites within organic and mineral nanopores [174]. This can enable the recovery of CH_4 from depleted natural gas reservoirs or coal seams and suggests a role for gas shales as GCS sites. Several groups have shown that gas sorption capacity is significantly greater in dry than moist clay rock (*e.g.*, [175]), although reports for CO_2 sorption in shale are conflicting [155]. Molecular simulations of gas mixtures are beginning both to reproduce trends in sorption affinity and to reveal molecular details of the competitive interactions [176]. Striolo and Cole have used molecular modeling to explore the structure and mobility of gas mixtures (including CO_2-butane, H_2O-ethanol) within idealized mineral pores [177-179]. Preferential sorption of one species to mineral surface sites can lead to an increase in the diffusivity of the second relative to that expected for a single phase system.

5.3 Sorption of cationic species

Within clay rock, sorption of cations on clay minerals is the main diffusion retardation factor. Clays and micas can retard cations through adsorption at edge sites and ion-exchange reactions with interlayer species [58, 150-153]. Dr. Garrison Sposito has written numerous papers and books on this topic, and the reader is referred to these excellent sources [3, 7, 56]. Figure 14 summarizes the continuum of different cation sorption mechanisms at work as a function of pH, at low ionic strength. (i) In pure cation exchange, the diffusing ion replaces the original species in a weak sorption site in the vicinity of the negatively charged clay basal layer. This site is an outer sphere complex in which a fully hydrated ion partly resides within a ditrigonal siloxane cavity. (ii) Certain cations (*e.g.*, Ni) undergo specific adsorption to specific edge sites, forming an inner sphere complex. (iii) The edge sites can also provide sites for epitaxial growth of metal silicates, as has been observed for Zn [58, 180-184].

Cationic species, e.g. Zn^{2+}, Ni^{2+}, Co^{2+}, Ba^{2+}, Fe^{2+} can also sorb on calcite [185, 186]. This phenomenon is often neglected due to the much larger specific surface are (and porosity) of clays

compared to carbonates.

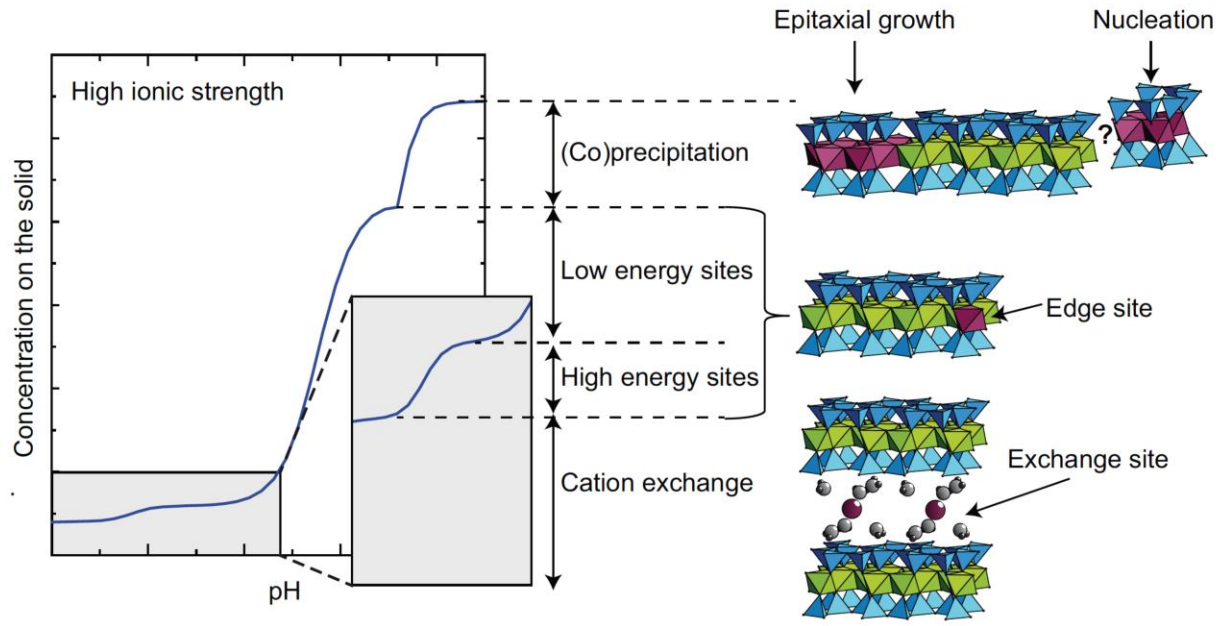

Figure 14 . *Relative importance of sorption processes on 2:1 clay minerals as a function of pH. Decreasing ionic strength results in a higher contribution of ion-exchange processes in the overall retention of cations (from [58])*

5.4 Sorption of anionic species

Iodine: I^- and ^{129}I

Iodide (I^-) is an example of a species that is present a low concentration, which sorbs weakly to most components of clay rock, but which can be immobilized by incorporation into precipitating carbonate phases. These factors make it challenging to predict the speciation and transport in clay rock. Clay rocks typically contain iodine at low concentration. In COx, for example, the total iodine natural geochemical background is very constant throughout the formation, with 1-5 mg I /kg in solid rock, and 20-40 µg I /L^{-1} in pore water [187]. Because negatively charged clays have an extremely weak affinity for iodine this natural content has been successively attributed to organic iodine [57, 188-190] or iodine present into carbonate shells [187, 191]. Spectroscopic studies that might distinguish between possible iodine species in clay rock (*e.g.*, I^-, IO_3^-, I_2 or organic iodine) have not been performed to date. Such studies will require careful preservation of the experimental pCO_2 at the value calculated for the host rock porewater in order to avoid carbonate dissolution or reprecipitation.

The radionuclide ^{129}Iodine is common in high-level radioactive wastes and has a long half-life (~$16x10^6$ years). Experiments of the diffusion of $^{125}I^-$ though Opalinus and Tournemire clay rock suggested that iodide migration is controlled by iodide retention on oxidized pyrite and natural organic matter [188-190]. When the CO_2 partial pressure is not controlled, a part of iodine is shown to be irreversibly bound to COx, probably in a newly precipitated carbonate phase [192]. Other ions such as selenite could be incorporated in calcite through similar mechanisms.

Selenium: SeO_3^{2-} and ^{79}Se

Selenium is naturally present in some clayrocks, associated with pyrite and organic matter. Flowback water from shale gas drilling operation commonly contain selenium, released after oxygen induced oxidation of host minerals and selenium species. The radionuclide ^{79}Se (half life ~10^6 years) is assumed to be released from reprocessing or spent fuel wastes in an oxidized state (VI or IV).

Selenium migration is strongly dependent on redox processes. The oxidized states of selenium form highly mobile oxyanions $Se(IV)O_3^{2-}$ and $Se(VI)O_4^{2-}$ in water while the lower oxidation states, Se(0) or Se(–II), are insoluble and hence less mobile.

In a radioactive waste storage (RWS) formation such as COx, with the likely presence of dissolved H_2, the Se(–II) state is most probable [193]. However, in Boom Clay [194-196], diffusion studies have shown Se to be prone to redox disequilibrium. As observed for sulfate, the thermodynamically reduction of SeO_4^{2-} does not occur unless process is catalyzed by microbial reactions or minerals. For example, in a low organic clay rock, such as Opalinus and Tournemire, Se retardation correlates with Fe(II) content [197]. Se(VI) reduction can occur through contact with Fe(II) including clay minerals [193], sulfide minerals [198] and with Fe(II) sorbed on calcite [199].

The diffusion Se(IV) can also be retarded by incorporation of selenite ion into carbonate minerals via coprecipitation and nearly isomorphic substitution during dynamic dissolution/precipitation phenomena (Figure 15) [200]. Indeed, selenite and carbonate ions have very similar structure and the substitution leads to a small but measurable (by XAS and neutron diffraction) expansion of the unit cell [201].

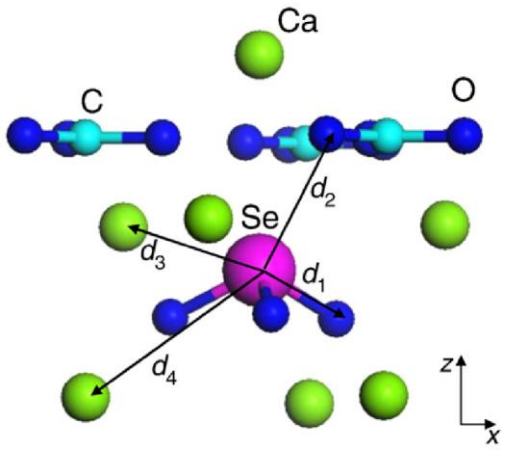

Figure 15*. Illustration of the structural site for the incorporation of selenite within calcite. Image from [201].*

Other species of concern

Clay rocks contain a range of minority elements or fluids that can negatively affect ecosystems if they are released through natural weathering processes or human activities. Flowback water from gas shales can contain volatile organics (such as ethane), toxic elements (such as ammonia, selenium, mercury, arsenic), as well as radioactive species (such as uranium, thorium and radium) [14]. Increasing disclosure of the chemical cocktails used for hydraulic fracturing has encouraged the use of more benign substances but some additives continue to be of concern [202].

6. Conclusions and Outlook

6.1 Basic research needs

The selection and use of low permeability sedimentary formations as repositories, barriers, cap rocks or other engineered systems requires reliable predictions of the transport of ions or molecules over time periods up to millennia. A substantial body of work on clays and clay rocks, briefly reviewed here, has achieved significant progress in describing diffusive transport through these nanoporous geologic media. Theoretical models that describe ion diffusion through electrical double layers and gas transport through inorganic pores appear to accurately depict the underlying physical processes. An important task is to obtain more realistic depictions of nanoporous transport pathways for gases and solutes, and to transfer the necessary multiscale

descriptions to computationally tractable large-scale modeling. Extension to clay rock formations containing insoluble organic matter will require additional work.

Reservoir-scale continuum modeling has provided important constraints on the effective diffusivity of natural tracers through sedimentary formations, but these approaches do not typically incorporate all the chemical processes that can significantly alter the mobility of species of concern. Processes such as sorption, ion exchange, dissolution/precipitation and microbiological processes are routinely handled with current reactive transport codes [203, 204],[205] but difficult to apply at the formation scale. Partly, this is an upscaling challenge with a lack of information on the connected porosity at the large scale, and on the mineral or organic phases defining this porosity. Partly, this is due to the lack of a molecular-scale, process-based description of relevant reactions and mineral surfaces within nanopores

The dynamic surface reactivity of carbonate minerals is especially important because these reactions can incorporate or release sorbates. Advances in these areas will require careful experiments with careful control of the partial pressures of O_2 and CO_2, which can control speciation and mineral incorporation reactions, respectively. Redox reactions can consume gaseous electron donors and acceptors and dramatically alter the mobility of key species. Establishing improved approaches to monitor gas and *E*h gradients in clay rock and signatures of past *E*h fluctuations will be of great value.

The relationships between pressure, pore morphology and transport are important to resolve even under conditions for which new fractures are not created. High-resolution imaging approaches that currently cannot be performed at relevant pressures could be complemented by scattering and sorption methods at a range of pressure to validate imaging results or perhaps to translate those observations into a high pressure regime. Many laboratory studies have provided rates of key mineral reactions that can create or fill pore space, such illitization or carbonate dissolution and cementation, but a long standing challenge is to translate lab measurements to natural systems. This challenge is especially severe for low-permeability rocks for which mineral reactions and solute transport through nanoscale pores is tightly coupled..

The grand challenge in this field is the demonstration that an accurate macroscopic prediction of transport can be built up from knowledge of clay rock composition and nano-to-mesoscale path

geometry. Achieving this connection between microscopic and macroscopic observations will require new creative approaches to link processes at different spatial and temporal scales [206]. Additional basic science challenges for successful use of these subsurface systems are summarized in a recent workshop report [207].

6.2 Clay rock community needs

In coming years, many nations will be developing policies that rely on sedimentary formations to achieve low-carbon or carbon-free energy goals. International collaboration and the use of experimental field observatories will be valuable to connect the best scientific research with geologic settings and engineering challenges. The Mont Terri site, pan-EU research programs such as FUNMIG (migration of radionuclides in clay rock), CATCLAY (cation transport in clays), RECOSY (redox processes in nuclear repositories), FORGE (gas migration), and international efforts such as DECOVALEX (DEvelopment of COupled models and their VALidation against EXperiments) have been models of international collaboration addressing the challenges for establishing a nuclear waste repository [208]. Additional regional collaborations would be valuable as other countries including many Asian nations (*e.g*. China South Korea and Japan) seek solutions for nuclear waste. Similarly the "The NEA Clay Club" working group on argillaceous media or the Clay Mineral Society have stimulated research and disseminated information to all aspects of the science and technology of clays (*e.g.*, [209])

The many properties and uses of clay rock also suggest the value of collaborative research with different focuses. In the US, for example, the Shale Hills Critical Zone Observatory [210] and The Marcellus Shale Energy and Environment Laboratory [211] are bringing diverse research teams together. Such interdisciplinary research will inform modern uses of sedimentary formations, knowledge of climate and terrestrial biological interactions with sedimentary rocks, and our understanding how biological records are altered by burial, decay and preservation.

Acknowledgments

We thank our three anonymous reviewers and many colleagues and collaborators including Christophe Tournassat, Ian Bourg, Carl Steefel, Jill Banfield, Martin Mazurek, Thomas Gimmi

and Luc Van Loon. L.C. has been supported for more than a decade by ANDRA. P.A-E is supported by the Swiss Competence Center for Energy Research (SCCER-SoE). P.W. has been supported by NAGRA for almost 20 years. B.G. was supported by the Center for Nanoscale Controls on Geologic CO_2 (NCGC), an Energy Frontier Research Center funded by the U.S. Department of Energy, Office of Science, Basic Energy Sciences under Award # DE-AC02-05CH11231.

References

1. Sposito, G. and R. Prost, *Structure of water adsorbed on smectites.* Chemical Reviews, 1982. **82**(552-573).
2. Greathouse, J.A., K. Refson, and G. Sposito, *Molecular dynamics simulation of water mobility in magnesium-smectite hydrates.* Journal of the American Chemical Society, 2000. **122**(46): p. 11459-11464.
3. Sposito, G., et al., *Surface geochemistry of the clay minerals.* Proceedings of the National Academy of Sciences of the United States of America, 1999. **96**(7): p. 3358-3364.
4. Bourg, I.C. and G. Sposito, *Connecting the Molecular Scale to the Continuum Scale for Diffusion Processes in Smectite-Rich Porous Media.* Environmental Science & Technology, 2010. **44**(6): p. 2085-2091.
5. Baryosef, B., et al., *Phorphorus adsorption by kaolinite and montmorillonite. 1. Effect of time, ionic strength and pH.* Soil Science Society of America Journal, 1988. **52**(6): p. 1580-1585.
6. Park, S.H. and G. Sposito, *Do montmorillonite surfaces promote methane hydrate formation? Monte Carlo and molecular dynamics simulations.* Journal of Physical Chemistry B, 2003. **107**(10): p. 2281-2290.
7. Sposito, G., *The Surface Chemistry of Soils*. 1984, New York: Oxford University Press.
8. Sposito, G., *Chemical Equilibria and Kinetics in Soils*. 1994: Oxford University Press.
9. Al, T., et al., *Geosynthesis: OPG's Deep Geologic Repository for Low and Intermediate Level Waste*. 2011.
10. Bock, H., et al., *Self-sealing of argillaceous formations in the context of geological disposal of radioactive waste*. 2010, OECD and NEA.
11. Rodwell, W., *A Thematic Network on Gas issues in Safety Assessment of Deep Repositories for Radioactive Waste (GASNET)*. 2003, European Commission: Luxemburg.
12. Shaw, R.P., ed. *Gas Generation and Migration. Proceedings of International Symposium and Workshop*. FORGE (Fate of Repository Gases) Project. 2013: Luxembourg.
13. Arthur, M.A. and D.R. Cole, *Unconventional hydrocarbon resources: prospects and problems.* Elements, 2014. **10**(4): p. 257-264.
14. Gregory, K.B., R.D. Vidic, and D.A. Dzombak, *Water management challenges associated with the production of shale gas by hydraulic fracturing.* Elements, 2011. **7**(3): p. 181-186.
15. Silin, D. and T. Kneafsey, *Shale gas: nanometer-scale observations and well modelling.* Journal of Canadian Petroleum Technology, 2012. **51**(6): p. 464-475.

16. Patzek, T.W., F. Male, and M. Marder, *Gas production in the Barnett Shale obeys a simple scaling theory.* Proceedings of the National Academy of Sciences of the United States of America, 2013. **110**(49): p. 19731-19736.
17. Vidic, R.D., et al., *Impact of shale gas development on regional water quality.* Science, 2013. **340**(6134).
18. Conley, S., et al., *Methane emissions from the 2015 Aliso Canyon blowout in Los Angeles, CA.* Science, 2016. **351**(6279): p. 1317-1320.
19. Kort, E.A., et al., *Fugitive emissions from the Bakken shale illustrate role of shale production in global ethane shift.* Geophysical Research Letters, 2016. **43**: p. 4617–4623.
20. Association), I.I.E., *CO2 Capture and Storage: a Key Carbon Abatement Option*. 2008: Paris.
21. Change), I.I.P.o.C., *Underground geological storage*, in *Special Report on Carbon Dioxide Capture and Storage*, B. Metz, et al., Editors. 2005.
22. Michael, K., et al., *Geological storage of CO2 in saline aquifers-A review of the experience from existing storage operations.* International Journal of Greenhouse Gas Control, 2010. **4**(4): p. 659-667.
23. Edlmann, K., et al., *Appraisal of global CO2 storage opportunities using the geomechanical facies approach.* Environmental Earth Sciences, 2015. **73**(12): p. 8075-8096.
24. White, J.A., et al., *Geomechanical behavior of the reservoir and caprock system at the In Salah CO2 storage project.* Proceedings of the National Academy of Sciences of the United States of America, 2014. **111**(24): p. 8747-8752.
25. Griffith, C.A., D.A. Dzombak, and G.V. Lowry, *Physical and chemical characteristics of potential seal strata in regions considered for demonstrating geological saline CO2 sequestration.* Environmental Earth Sciences, 2011. **64**: p. 925-948.
26. Lu, J., et al., *Reservoir characterization and complications for trapping mechanisms at Cranfield CO2 injection site.* International Journal of Greenhouse Gas Control, 2013. **18**: p. 361-374.
27. Song, J. and D. Zhang, *Comprehensive review of caprock-sealing mechanisms for geologic carbon sequestration.* Environmental Science & Technology, 2013. **47**(1): p. 9-22.
28. Shao, H., et al., *Mobilization of metals from Eau Claire siltstone and the impact of oxygen under geological carbon dioxide sequestration conditions.* Geochimica Et Cosmochimica Acta, 2014. **141**: p. 62-82.
29. Kampman, N., et al., *Drilling and sampling a natural CO2 reservoir: Implications for fluid flow and CO2-fluid-rock reactions during CO2 migration through the overburden.* Chemical Geology, 2014. **369**: p. 51-82.
30. Carden, P.O. and L. Paterson, *Physical, chemical and energy aspects of underground hydrogen storage.* International Journal of Hydrogen Energy, 1979. **4**: p. 559-569.
31. Stone, H.B.J., I. Velduis, and N. Richardson, *Underground hydrogen storage in the UK*, in *Underground Gas Storage: Worldwide Experiences and Future Developments in the UK and Europe*, D.R. Evans and R.A. Chadwick, Editors. 2009, The Geological Society: London. p. 217-226.
32. Lord, A.S., et al., *A life cycle cost analysis framework for geologic storage of hydrogen: a user's tool*. 2011, Sandia National Laboratories.

33. Oladyshkin, S. and M. Panfilov, *Hydrogen penetration in water through porous medium: application to a radioactive waste storage site.* Environmental Earth Sciences, 2011. **64**(4): p. 989-999.
34. Brantley, S.L., et al., *Probing deep weathering in the Shale Hills Critical Zone Observatory, Pennsylvania (USA): the hypothesis of nested chemical reaction fronts in the subsurface.* Earth Surface Processes and Landforms, 2013. **38**(11): p. 1280-1298.
35. Suchet, P.A., J.L. Probst, and W. Ludwig, *Worldwide distribution of continental rock lithology: Implications for the atmospheric/soil CO2 uptake by continental weathering and alkalinity river transport to the oceans.* Global Biogeochemical Cycles, 2003. **17**(2).
36. Morrison, S.J., et al., *Naturally occurring contamination in the Mancos Shale.* Environmental Science & Technology, 2012. **46**(3): p. 1379-1387.
37. Strathouse, S.M., et al., *Geologic nitrogen - a potential geochemical hazard in the San-Joaquin Valley, California.* Journal of Environmental Quality, 1980. **9**(1): p. 54-60.
38. Morris, S.C., *Burgess shale faunas and the Cambrian explosion.* Science, 1989. **246**(4928): p. 339-346.
39. Tian, S.G., et al., *Sequence stratigraphy of Jurassic-Cretaceous boundary strata in Luanping, northern Hebei, China.* Science in China Series D-Earth Sciences, 2004. **47**(7): p. 607-617.
40. Wang, M., et al., *The oldest record of ornithuromorpha from the early cretaceous of China.* Nature Communications, 2015. **6**.
41. Ashton, N., et al., *Hominin Footprints from Early Pleistocene Deposits at Happisburgh, UK.* Plos One, 2014. **9**(2).
42. Mitchell, K., et al., *Selenium as paleo-oceanographic proxy: A first assessment.* Geochimica Et Cosmochimica Acta, 2012. **89**: p. 302-317.
43. von Strandmann, P.A.E.P., et al., *Selenium isotope evidence for progressive oxidation of the Neoproterozoic biosphere.* Nature Communications, 2015. **6**.
44. Chermak, J.A. and M.E. Schreiber, *Mineralogy and trace element geochemistry of gas shales in the United States.* International Journal of Coal Geology, 2014. **126**: p. 32-44.
45. Damste, J.S.S., et al., *A 6,000-year sedimentary molecular record of chemocline excursions in the Black Sea.* Nature, 1993. **362**(6423): p. 827-829.
46. Berner, R.A., *Early Diagenesis: A Theoretical Approach*. 1980: Princeton University Press.
47. Taylor, K.G. and J.H.S. Macquaker, *Diagenetic alterations in a silt- and clay-rich mudstone succession: an example from the Upper Cretaceous Mancos Shale of Utah, USA.* Clay Minerals, 2014. **49**(2): p. 213-227.
48. Lazar, O.R., et al., *Capturing key attributes of fine-grained sedimentary rocks in outcrops, cores, and thin sections: nomeclature and description guidelines.* Journal of Sedimentary Research, 2015. **85**(3): p. 230-246.
49. Gaucher, E., et al., *ANDRA underground research laboratory: interpretation of the mineralogical and geochemical data acquired in the Callovian-Oxfordian formation by investigative drilling.* Physics and Chemistry of the Earth, 2004. **29**(1): p. 55-77.
50. Hama, K., et al., *The hydrogeochemistry of argillaceous rock formations at the Horonobe URL site, Japan.* Physics and Chemistry of the Earth, 2007. **32**(1-7): p. 170-180.
51. Rickman, R., et al., *A practical use of shale petrophysics for stimulation design optimization: all shale plays are not clones of the Barnett Shale.* SPE International, 2008. **115258**: p. 1-11.

52. Fisher, Q., F. Kets, and A. Crook, *Self-sealing of faults and fractures in argillaceous formations: Evidence from the petroleum industry*. 2013, NAGRA.
53. Blanc, P., O. Legendre, and E.C. Gaucher, *Estimate of clay minerals amounts from XRD pattern modeling: The Arquant model.* Physics and Chemistry of the Earth, 2007. **32**(1-7): p. 135-144.
54. Gaucher, E.C. and P. Blanc, *Cement/clay interactions - A review: Experiments, natural analogues, and modeling.* Waste Management, 2006. **26**(7): p. 776-788.
55. Thyberg, B., et al., *Quartz cementation in Late Cretaceous mudstones, northern North Sea: Changes in rock properties due to dissolution of smectite and precipitation of micro-quartz crystals.* Marine and Petroleum Geology, 2010. **27**(8): p. 1752-1764.
56. Sposito, G., *The thermodynamics of soil solutions*. 1981: Oxford University Press.
57. Tournassat, C., et al., *On the mobility and potential retention of iodine in the Callovian-Oxfordian formation.* Physics and Chemistry of the Earth, 2007. **32**(8-14): p. 539-551.
58. Tournassat, C., et al., *Modeling specific pH dependent sorption of divalent metals on montmorillonite surfaces. A review of pitfalls, recent achievements and current challenges.* American Journal of Science, 2013. **313**(5): p. 395-451.
59. Tournassat, C. and C.I. Steefel, *Ionic transport in nano-porous clays with consideration of electrostatic effects*, in *Pore-Scale Geochemical Processes*, C.I. Steefel, S. Emmanuel, and L.M. Anovitz, Editors. 2015. p. 287-329.
60. Jaynes, W.F. and S.A. Boyd, *Hydrophobicity of siloxane surfaces in smectites as revealed by aromatic hydrocarbon adsorption from water.* Clays and Clay Minerals, 1991. **39**(4): p. 428-436.
61. Rotenberg, B., A.J. Patel, and D. Chandler, *Molecular explanation for why talc surfaces can be both hydrophilic and hydrophobic.* Journal of the American Chemical Society, 2011. **133**(50): p. 20521-20527.
62. Ferrage, E., et al., *Hydration Properties and Interlayer Organization of Water and Ions in Synthetic Na-Smectite with Tetrahedral Layer Charge. Part 2. Toward a Precise Coupling between Molecular Simulations and Diffraction Data.* Journal of Physical Chemistry C, 2011. **115**(5): p. 1867-1881.
63. Dazas, B., et al., *Influence of tetrahedral layer charge on the organization of interlayer water and ions in synthetic Na-saturated smectites.* Journal of Physical Chemistry C, 2015. **119**(8): p. 4158-4172.
64. Low, P.F. and J.F. Margheim, *Swelling of clay. 1. Basic concepts and empirical equations.* Soil Science Society of America Journal, 1979. **43**(3): p. 473-481.
65. Anderson, R.L., et al., *Clay swelling — a challenge in the oilfield.* Earth-Science Reviews, 2010. **98**: p. 201-216.
66. Wersin, P., E. Curti, and C.A.J. Appelo, *Modelling bentonite-water interactions at high solid/liquid ratios: swelling and diffuse double layer effects.* Applied Clay Science, 2004. **26**(1-4): p. 249-257.
67. Zanella, A., P.R. Cobbold, and T. Boassen, *Natural hydraulic fractures in the Wessex Basin, SW England: Widespread distribution, composition and history.* Marine and Petroleum Geology, 2015. **68**: p. 438-448.
68. Tournassat, C., et al., *Chemical conditions in clay rocks*. 2015, Elsevier.
69. Gaucher, E.C., et al., *Modelling the porewater chemistry of the Callovian-Oxfordian formation at a regional scale.* Comptes Rendus Geoscience, 2006. **338**(12-13): p. 917-930.

70. Tournassat, C., et al., *Cation exchanged Fe(II) and Sr compared to other divalent cations (Ca, Mg) in the bure Callovian-Oxfordian formation: Implications for porewater composition modelling.* Applied Geochemistry, 2008. **23**(4): p. 641-654.
71. Kars, M., et al., *Identification of nanocrystalline goethite in reduced clay formations: Application to the Callovian-Oxfordian formation of Bure (France).* American Mineralogist, 2015. **100**(7): p. 1544-1553.
72. Vandenbroucke, M. and C. Largeau, *Kerogen origin, evolution and structure.* Organic Geochemistry, 2007. **38**: p. 719-833.
73. Grasset, L., et al., *Sequential extraction and spectroscopic characterisation of organic matter from the Callovo-Oxfordian formation.* Organic Geochemistry, 2010. **41**(3): p. 221-233.
74. Slatt, R.M. and N.R. O'Brien, *Pore types in the Barnett and Woodford gas shales: Contribution to understanding gas storage and migration pathways in fine-grained rocks.* Aapg Bulletin, 2011. **95**(12): p. 2017-2030.
75. Romero-Sarmiento, M.-F., et al., *Evolution of Barnett Shale organic carbon structure and nanostructure with increasing maturation.* Organic Geochemistry, 2014. **71**: p. 7-16.
76. Courdouan, A., et al., *Isolation and characterization of dissolved organic matter from the Callovo-Oxfordian formation.* Applied Geochemistry, 2007. **22**(7): p. 1537-1548.
77. Huclier-Markai, S., et al., *Non-disturbing characterization of natural organic matter (NOM) contained in clay rock pore water by mass spectrometry using electrospray and atmospheric pressure chemical ionization modes.* Rapid Communications in Mass Spectrometry, 2010. **24**(2): p. 191-202.
78. Fernandez, A.M., et al., *Applying the squeezing technique to highly consolidated clayrocks for pore water characterisation: Lessons learned from experiments at the Mont Terri Rock Laboratory.* Applied Geochemistry, 2014. **49**: p. 2-21.
79. Bruggeman, C. and M. De Craen, *Boom Clay natural organic matter. Status Report 2011*. 2012: Mol, Belgium.
80. Courdouan, A., et al., *Characterization of dissolved organic matter in anoxic rock extracts and in situ pore water of the Opalinus Clay.* Applied Geochemistry, 2007. **22**(12): p. 2926-2939.
81. Martens, E., et al., *Modelling of a large-scale in-situ migration experiment with 14C-labelled natural organic matter in Boom Clay.* Radiochimica Acta, 2010. **89**: p. 695–701.
82. Maes, N., et al., *A consistent phenomenological model for natural organic matter linked migration of Tc(IV), Cm(III), Np(IV), Pu(III/IV) and Pa(V) in the Boom Clay.* Physics and Chemistry of the Earth, 2011. **36**(17-18): p. 1590-1599.
83. Maes, N., et al., *The role of natural organic matter in the migration behaviour of americium in the Boom Clay - Part I: Migration experiments.* Physics and Chemistry of the Earth, 2006. **31**(10-14): p. 541-547.
84. Courdouan, A., et al., *Proton and trivalent metal cation binding by dissolved organic matter in the Opalinus Clay and the Callovo-Oxfordian formation.* Environmental Science & Technology, 2008. **42**(16): p. 5985-5991.
85. Hummel, W., M.A. Glaus, and L.R. Van Loon, *Trace metal-humate interactions. II. The "conservative roof" model and its application.* Applied Geochemistry, 2000. **15**(7): p. 975-1001.
86. Ougier-Simonin, A., et al., *Microfracturing and microporosity in shales.* Earth-Science Reviews, 2016. **162**: p. 198-226.

87. Bourg, I.C., *Sealing shales versus brittle shales: a sharp threshold in the material properties and energy technology uses of fine-grained sedimentary rocks.* Environmental Science & Technology Letters, 2015. **2**(10): p. 255-259.
88. Crawford, B.R., D.R. Faulkner, and E.H. Rutter, *Strength, porosity, and permeability development during hydrostatic and shear loading of synthetic quartz-clay fault gouge.* Journal of Geophysical Research-Solid Earth, 2008. **113**(B3).
89. David, C., et al., *Laboratory measurement of compaction-induced permeability change in porous rocks - implications for the generation and maintenance of pore pressure excess in the crust.* Pure and Applied Geophysics, 1994. **143**(1-3): p. 425-456.
90. Zhang, R., et al., *Impacts of nanopore structure and elastic properties on stress-dependent permeability of gas shales.* Journal of Natural Gas Science and Engineering, 2015. **26**: p. 1663-1672.
91. Harrington, J.F., et al., *Laboratory study of gas and water flow in the Nordland shale, Sleipner, North Sea*, in *Carbon dioxide sequestration in geological media—State of the science*, E. Grobe, J.C. Pashin, and R.L. Dodge, Editors. 2009. p. 521-543.
92. Bachaud, P., et al., *Use of tracers to characterize the effects of a CO2-saturated brine on the petrophysical properties of a low permeability carbonate caprock.* Chemical Engineering Research & Design, 2011. **89**(9): p. 1817-1826.
93. Wang, G., et al., *Identifying organic-rich Marcellus Shale lithofacies by support vector machine classifier in the Appalachian basin.* Computers & Geosciences, 2014. **64**: p. 52-60.
94. Robinet, J.-C., et al., *Effects of mineral distribution at mesoscopic scale on solute diffusion in a clay-rich rock: Example of the Callovo-Oxfordian mudstone (Bure, France).* Water Resources Research, 2012. **48**.
95. Boyer, D.L., E.E. Haddad, and E.S. Seeger, *The last gasp: trace fossils track deoxygenation leading into the Frasnian-Famennian extinction event.* Palaios, 2014. **29**(12): p. 646-651.
96. Tournassat, C., et al., *Nanomorphology of montmorillonite particles: Estimation of the clay edge sorption site density by low-pressure gas adsorption and AFM observations.* American Mineralogist, 2003. **88**(11-12): p. 1989-1995.
97. Keller, L.M., et al., *Characterization of multi-scale microstructural features in Opalinus Clay.* Microporous and Mesoporous Materials, 2013. **170**: p. 83-94.
98. Song, Y., et al., *Multi-scale pore structure of COx claystone: Towards the prediction of fluid transport.* Marine and Petroleum Geology, 2015. **65**: p. 63-82.
99. King, H.E., Jr., et al., *Pore architecture and connectivity in gas shale.* Energy & Fuels, 2015. **29**(3): p. 1375-1390.
100. Bernard, S., et al., *Geochemical evolution of organic-rich shales with increasing maturity: A STXM and TEM study of the Posidonia Shale (Lower Toarcian, northern Germany).* Marine and Petroleum Geology, 2012. **31**(1): p. 70-89.
101. Gilbert, B., et al., *Formation and restacking of disordered smectite osmotic hydrates.* Clays and Clay Minerals, 2015. **63**(6): p. 432-442.
102. Swift, A.M., et al., *Relationship between mineralogy and porosity in seals relevant to geologic CO2 sequestration.* Environmental Geosciences, 2014. **2**: p. 39-57.
103. Gaboreau, S., J.-C. Robinet, and D. Pret, *Optimization of pore-network characterization of a compacted clay material by TEM and FIB/SEM imaging.* Microporous and Mesoporous Materials, 2016. **224**: p. 116-128.

104. Gu, X., et al., *Pores in Marcellus Shale: a neutron scattering and FIB-SEM study.* Energy & Fuels, 2015. **29**(3): p. 1295-1308.
105. Kuila, U., et al., *Nano-scale texture and porosity of organic matter and clay minerals in organic-rich mudrocks.* Fuel, 2014. **135**: p. 359-373.
106. Chalmers, G.R., R.M. Bustin, and I.M. Power, *Characterization of gas shale pore systems by porosimetry, pycnometry, surface area, and field emission scanning electron microscopy/transmission electron microscopy image analyses: Examples from the Barnett, Woodford,Haynesville, Marcellus, and Doig units.* AAPG Bulletin, 2012. **96**: p. 1099-1119.
107. Schaefer, T., et al., *Radiation sensitivity of natural organic matter: Clay mineral association effects in the Callovo-Oxfordian argillite.* Journal of Electron Spectroscopy and Related Phenomena, 2009. **170**(1-3): p. 49-56.
108. Wise, A.M., et al., *Nanoscale chemical imaging of an individual catalyst particle with soft X-ray ptychography.* Acs Catalysis, 2016. **6**(4): p. 2178-2181.
109. Hu, Q., R.P. Ewing, and S. Dultz, *Low pore connectivity in natural rock.* Journal of Contaminant Hydrology, 2012. **133**: p. 76-83.
110. Neuzil, C.E., *How permeable are clays and shales?* Water Resources Research, 1994. **30**(2): p. 145-150.
111. Mazurek, M., et al., *Natural tracer profiles across argillaceous formations.* Applied Geochemistry, 2011. **26**(7): p. 1035-1064.
112. Yang, Y. and A.C. Aplin, *A permeability-porosity relationship for mudstones.* Marine and Petroleum Geology, 2010. **27**(8): p. 1692-1697.
113. Grunau, H.R., *A worldwide look at the cap-rock problem.* Journal of Petroleum Geology, 1987. **10**: p. 245-266.
114. Chagneau, A., et al., *Complete restriction of Cl-36(-) diffusion by celestite precipitation in densely compacted illite.* Environmental Science & Technology Letters, 2015. **2**(5): p. 139-143.
115. Mazurek, M., et al., *Transferability of geoscientific information from various sources (study sites, underground rock laboratories, natural analogues) to support safety cases for radioactive waste repositories in argillaceous formations.* Physics and Chemistry of the Earth, 2008. **33**: p. S95-S105.
116. Van Loon, L.R. and J. Mibus, *A modified version of Archie's law to estimate effective diffusion coefficients of radionuclides in argillaceous rocks and its application in safety analysis studies.* Applied Geochemistry, 2015. **59**: p. 85-94.
117. Cygan, R.T., *The Solubility of Gases in NaCl Brine and a Critical Evaluation of Available Data*. 1991, Sandia: Albuquerque, New Mexico.
118. Gyoere, D., et al., *Tracing injected CO2 in the Cranfield enhanced oil recovery field (MS, USA) using He, Ne and Ar isotopes.* International Journal of Greenhouse Gas Control, 2015. **42**: p. 554-561.
119. Van Loon, L.R., M.A. Glaus, and W. Mueller, *Anion exclusion effects in compacted bentonites: Towards a better understanding of anion diffusion.* Applied Geochemistry, 2007. **22**(11): p. 2536-2552.
120. Mazurek, M., et al., *Natural Tracer Profiles across Argillaceous Formations: The CLAYTRAC Project*. 2009, OECD Nuclear Energy Agency: Paris.

121. Soler, J.M., *The effect of coupled transport phenomena in the Opalinus Clay and implications for radionuclide transport.* Journal of Contaminant Hydrology, 2001. **53**(1-2): p. 63-84.
122. Goncalves, J., et al., *Semipermeable Membrane Properties and Chemomechanical Coupling in Clay Barriers*. 2015, Elsevier.
123. Tournassat, C., et al., *Molecular dynamics simulations of anion exclusion in clay interlayer nanopores.* Geochimica Et Cosmochimica Acta, 2016. **in press**.
124. Charlet, L. and C. Tournassat, *Fe(II)-Na(I)-Ca(II) cation exchange on montmorillonite in chloride medium: Evidence for preferential clay adsorption of chloride - Metal ion pairs in seawater.* Aquatic Geochemistry, 2005. **11**(2): p. 115-137.
125. Sposito, G., et al., *Sodium calcium and sodium magnesium exchange on Wyoming bentonite in perchlorate and chloride background ionic media.* Soil Science Society of America Journal, 1983. **47**(1): p. 51-56.
126. Ferrage, E., et al., *Experimental evidence for Ca-chloride ion pairs in the interlayer of montmorillonite. An XRD profile modeling approach.* Clays and Clay Minerals, 2005. **53**(4): p. 348-360.
127. Gebauer, D., A. Völkel, and H. Cölfen, *Stable prenucleation calcium carbonate clusters.* Science, 2008. **322**: p. 1819-1822.
128. Tournassat, C., et al., *Molecular dynamics simulations of anions exclusion in clay interlayer nanopores.* Clays and Clay Minerals, 2016. **64**(4): p. 374-388.
129. Sanchez, F.G., et al., *Linking the diffusion of water in compacted clays at two different time scales: tracer through-diffusion and quasielastic neutron scattering.* Environmental Science & Technology, 2009. **43**: p. 3487-3493.
130. Zarzycki, P. and B. Gilbert, *Long-range interactions restrict water transport in pyrophyllite interlayers.* Scientific Reports, 2016. **6**.
131. Tertre, E., et al., *Cation diffusion in the interlayer space of swelling clay minerals - A combined macroscopic and microscopic study.* Geochimica Et Cosmochimica Acta, 2015. **149**: p. 251-267.
132. Tinnacher, R.M., et al., *Ion adsorption and diffusion in smectite: Molecular, pore, and continuum scale views.* Geochimica Et Cosmochimica Acta, 2016. **177**: p. 130-149.
133. Maes, N., et al., *Migration Case Study: Transport of Radionuclides in a Reducing Clay Sediment (TRANCOM-II)*. 2004: Mol, Belgium.
134. Voegelin, A. and R. Kretzschmar, *Stability and mobility of colloids in Opalinus Clay*. 2002: Wettingen.
135. Marschall, P., S. Horseman, and T. Gimmi, *Characterisation of gas transport properties of the Opalinus clay, a potential host rock formation for radioactive waste disposal.* Oil & Gas Science and Technology-Revue D Ifp Energies Nouvelles, 2005. **60**(1): p. 121-139.
136. Amann-Hildenbrand, A., et al., *Gas Transfer Through Clay Barriers*, in *Developments in Clay Science*, C. Tournassat, et al., Editors. 2015, Elsevier.
137. Trebotich, D., et al., *High-resolution simulation of pore-scale reactive transport processes associated with carbon sequestration.* Computing in Science & Engineering, 2014. **16**(6): p. 22-31.
138. Ziarani, A.S. and R. Aguilera, *Knudsen's permeability correction for tight porous media.* Transport in Porous Media, 2012. **91**(1): p. 239-260.

139. Javadpour, F., D. Fisher, and M. Unsworth, *Nanoscale gas flow in shale gas sediments.* Journal of Canadian Petroleum Technology, 2007. **46**(10): p. 55-61.
140. Cui, X., A.M.M. Bustin, and R.M. Bustin, *Measurements of gas permeability and diffusivity of tight reservoir rocks: different approaches and their applications.* Geofluids, 2009. **9**(3): p. 208-223.
141. Marschall, P., S. Horseman, and T. Gimmi, *Characterisation of gas transport properties of the Opalinus clay, a potential host rock formation for radioactive waste disposal.* Oil & Gas Science and Technology, 2005. **60**: p. 121-139.
142. Jacops, E., et al., *Measuring the effective diffusion coefficient of dissolved hydrogen in saturated Boom Clay.* Applied Geochemistry, 2015. **61**: p. 175-184.
143. Bensenouci, F., et al., *Profiles of chloride and stable isotopes in pore-water obtained from a 2000 m-deep borehole through the Mesozoic sedimentary series in the eastern Paris Basin.* Physics and Chemistry of the Earth, 2013. **65**: p. 1-10.
144. Sasamoto, H., R.C. Arthur, and K. Hama, *Interpretation of undisturbed hydrogeochemical conditions in Neogene sediments of the Horonobe area, Hokkaido, Japan.* Applied Geochemistry, 2011. **26**(8): p. 1464-1477.
145. B., M. and B. J., *La démarche scientifique de l'Andra: site du Gard: In: Etude du Gard Rhodanien*, in *Etude du Gard Rhodanien. Actes des journées scientifiques CNRS/Andra, Bagnols-sur Cèze, 20 et 21 octobre 1997*. 1999, EDP Sciences: Les Ulis, France. p. 167-187.
146. Wersin, P., et al., *Long-term diffusion experiment at Mont Terri: first results from field and laboratory data.* Applied Clay Science, 2004. **26**(1-4): p. 123-135.
147. Delay, J., et al., *Scientific investigation in deep wells for nuclear waste disposal studies at the Meuse/Haute Marne underground research laboratory, Northeastern France.* Physics and Chemistry of the Earth, 2007. **32**(1-7): p. 42-57.
148. Bensenouci, F., et al., *Coupled study of water-stable isotopes and anions in porewater for characterizing aqueous transport through the Mesozoic sedimentary series in the eastern Paris Basin.* Marine and Petroleum Geology, 2014. **53**: p. 88-101.
149. Kurikami, H., R. Takeuchi, and S. Yabuuchi, *Scale effect and heterogeneity of hydraulic conductivity of sedimentary rocks at Horonobe URL site.* Physics and Chemistry of the Earth, 2008. **33**: p. S37-S44.
150. Fletcher, P., et al., *Sodium-calcium-magnesium exchange-reactions on a montmorillonitic soil. 2. Ternary-exchange reactions.* Soil Science Society of America Journal, 1984. **48**(5): p. 1022-1025.
151. Fletcher, P., G. Sposito, and C.S. Levesque, *Sodium-calcium-magnesium exchange-reactions on a montmorillonitic soil. 1. Binary exchange-reactions.* Soil Science Society of America Journal, 1984. **48**(5): p. 1016-1021.
152. Baeyens, B. and M.H. Bradbury, *A mechanistic description of Ni and Zn sorption on Na-montmorillonite .1. Titration and sorption measurements.* Journal of Contaminant Hydrology, 1997. **27**(3-4): p. 199-222.
153. Bradbury, M.H. and B. Baeyens, *A mechanistic description of Ni and Zn sorption on Na-montmorillonite .2. Modelling.* Journal of Contaminant Hydrology, 1997. **27**(3-4): p. 223-248.
154. Stack, A.G., et al., *Pore-size-dependent calcium carbonate precipitation controlled by surface chemistry.* Environmental Science & Technology, 2014. **48**(11): p. 6177-6183.

155. Busch, A., et al., *Carbon dioxide storage potential of shales.* International Journal of Greenhouse Gas Control, 2008. **2**(3): p. 297-308.
156. de Jong, S.M., C.J. Spiers, and A. Busch, *Development of swelling strain in smectite clays through exposure to carbon dioxide.* International Journal of Greenhouse Gas Control, 2014. **24**: p. 149-161.
157. Schaef, H.T., et al., *Competitive sorption of CO2 and H2O in 2:1 layer phyllosilicates.* Geochimica Et Cosmochimica Acta, 2015. **161**: p. 248-257.
158. Michels, L., et al., *Intercalation and retention of carbon dioxide in a smectite clay promoted by interlayer cations.* Scientific Reports, 2015. **5**.
159. Wan, J., Y. Kim, and T.K. Tokunaga, *Contact angle measurement ambiguity in supercritical CO2-water-mineral systems: Mica as an example.* International Journal of Greenhouse Gas Control, 2014. **31**: p. 128-137.
160. Hur, T.-B., et al., *Carbonate formation in Wyoming montmorillonite under high pressure carbon dioxide.* International Journal of Greenhouse Gas Control, 2013. **13**: p. 149-155.
161. Andreani, M., et al., *Changes in seal capacity of fractured claystone caprocks induced by dissolved and gaseous CO(2) seepage.* Geophysical Research Letters, 2008. **35**(14).
162. Ross, D.J.K. and R.M. Bustin, *The importance of shale composition and pore structure upon gas storage potential of shale gas reservoirs.* Marine and Petroleum Geology, 2009. **26**(6): p. 916-927.
163. Zhang, T., et al., *Effect of organic-matter type and thermal maturity on methane adsorption in shale-gas systems.* Organic Geochemistry, 2012. **47**: p. 120-131.
164. Bousige, C., et al., *Realistic molecular model of kerogen's nanostructure.* Nature Materials, 2016. **15**(5): p. 576-+.
165. Liu, K., et al., *Molecular simulation of gas adsorption in minerals and coal: Implications for gas occurrence in shale gas reservoirs*, in *Fundamentals of Gas Shale Reservoirs*, R. Rezaee, Editor. 2015, John Wiley & Sons, Ltd.: Hoboken, New Jersey, USA.
166. Titiloye, J.O. and N.T. Skipper, *Computer simulation of the structure and dynamics of methane in hydrated Na-smectite clay.* Chemical Physics Letters, 2000. **329**(1-2): p. 23-28.
167. Titiloye, J.O. and N.T. Skipper, *Monte Carlo and molecular dynamics simulations of methane in potassium montmorillonite clay hydrates at elevated pressures and temperatures.* Journal of Colloid and Interface Science, 2005. **282**: p. 422-427.
168. Vinsot, A., et al., *In situ diffusion test of hydrogen gas in the Opalinus Clay*, in *Clays in Natural and Engineered Barriers for Radioactive Waste Confinement*, S. Norris, et al., Editors. 2014, Geological Society, London.
169. Bagnoud, A., et al., *Rates of microbial hydrogen oxidation and sulfate reduction in Opalinus Clay rock.* Applied Geochemistry, 2016. **72**: p. 42-50.
170. Bardelli, F., et al., *Hydrogen uptake and diffusion in Callovo-Oxfordian clay rock for nuclear waste disposal technology.* Applied Geochemistry, 2014. **49**: p. 168-177.
171. Didier, M., et al., *Adsorption of hydrogen gas and redox processes in clays.* Environmental Science & Technology, 2012. **46**(6): p. 3574-3579.
172. Mondelli, C., et al., *Hydrogen adsorption and diffusion in synthetic Na-montmorillonites at high pressures and temperature.* International Journal of Hydrogen Energy, 2015. **40**(6): p. 2698-2709.

173. Edge, J.S., et al., *Structure and dynamics of molecular hydrogen in the interlayer pores of a swelling 2:1 clay by neutron scattering.* Journal of Physical Chemistry C, 2014. **118**(44): p. 25740-25747.
174. Bacon, D.H., et al., *CO2 storage by sorption on organic matter and clay in gas shale.* Journal of Unconventional Oil and Gas Resources, 2015. **12**: p. 123-33.
175. Yuan, W., et al., *Experimental study and modelling of methane adsorption and diffusion in shale.* Fuel, 2014. **117**: p. 509-519.
176. Yang, N., S. Liu, and X. Yang, *Molecular simulation of preferential adsorption of CO2 over CH4 in Na-montmorillonite clay material.* Applied Surface Science, 2015. **356**: p. 1262-1271.
177. Anh, P., D.R. Cole, and A. Striolo, *Preferential adsorption from liquid water-ethanol mixtures in alumina pores.* Langmuir, 2014. **30**(27): p. 8066-8077.
178. Le, T., A. Striolo, and D.R. Cole, *CO2-C4H10 mixtures simulated in silica slit pores: relation between structure and dynamics.* Journal of Physical Chemistry C, 2015. **119**(27): p. 15274-15284.
179. Phan, A., D.R. Cole, and A. Striolo, *Factors governing the behaviour of aqueous methane in narrow pores.* Philosophical Transactions of the Royal Society a-Mathematical Physical and Engineering Sciences, 2016. **374**(2060).
180. Tournassat, C., et al., *The titration of clay minerals II. Structure-based model and implications for clay reactivity.* Journal of Colloid and Interface Science, 2004. **273**(1): p. 234-246.
181. Tournassat, C., et al., *Cation exchange selectivity coefficient values on smectite and mixed-layer illite/smectite minerals.* Soil Science Society of America Journal, 2009. **73**(3): p. 928-942.
182. Schlegel, M.L., et al., *Adsorption mechanisms of Zn on hectorite as a function of time, pH, and ionic strength.* American Journal of Science, 2001. **301**(9): p. 798-830.
183. Schlegel, M.L., et al., *Sorption of metal ions on clay minerals I. Polarized EXAFS evidence for the adsorption of Co on the edges of hectorite particles.* Journal of Colloid and Interface Science, 1999. **215**(1): p. 140-158.
184. Charlet, L. and A. Manceau, *Evidence for the neoformation of clays upon sorption of Co(II) and Ni(II) on silicates.* Geochimica Et Cosmochimica Acta, 1994. **58**(11): p. 2577-2582.
185. Zachara, J.M., C.E. Cowan, and C.T. Resch, *Sorption of divalent metals on calcite.* Geochimica Et Cosmochimica Acta, 1991. **55**(6): p. 1549-1562.
186. Mettler, S., et al., *Sorption and catalytic oxidation of Fe(II) at the surface of calcite.* Geochimica Et Cosmochimica Acta, 2009. **73**(7): p. 1826-1840.
187. Claret, F., et al., *Natural iodine in a clay formation: Implications for iodine fate in geological disposals.* Geochimica Et Cosmochimica Acta, 2010. **74**(1): p. 16-29.
188. Savoye, S., et al., *How mobile is iodide in the Callovo-Oxfordian claystones under experimental conditions close to the in situ ones?* Journal of Contaminant Hydrology, 2012. **142**: p. 82-92.
189. Wittebroodt, C., et al., *Diffusion of HTO, Cl-36(-) and I-125(-) in Upper Toarcian argillite samples from Tournemire: Effects of initial iodide concentration and ionic strength.* Applied Geochemistry, 2012. **27**(7): p. 1432-1441.

190. Frasca, B., et al., *Influence of redox conditions on iodide migration through a deep clay formation (Toarcian argillaceous rock, Tournemire, France).* Applied Geochemistry, 2012. **27**(12): p. 2453-2462.
191. Lerouge, C., et al., *Comparative EPMA and mu-XRF methods for mapping micro-scale distribution of iodine in biocarbonates of the Callovian-Oxfordian clayey formation at Bure, Eastern part of the Paris Basin.* Physics and Chemistry of the Earth, 2010. **35**(6-8): p. 271-277.
192. Montavon, G., et al., *Retention of iodide by the Callovo-Oxfordian formation: An experimental study.* Applied Clay Science, 2014. **87**: p. 142-149.
193. Charlet, L., et al., *Electron transfer at the mineral/water interface: Selenium reduction by ferrous iron sorbed on clay.* Geochimica Et Cosmochimica Acta, 2007. **71**(23): p. 5731-5749.
194. Beauwens, T., et al., *Studying the migration behaviour of selenate in Boom Clay by electromigration.* Engineering Geology, 2005. **77**(3-4): p. 285-293.
195. Bruggeman, C., *Assessment of the geochemical behviour of selenium oxyaniions under Boom Clay geochemical conditions*. 2006, Katholieke Universiteit Leuven.
196. De Cannière, P., et al., *Behavioiur of selenium in Boom Clay*. 2010: Mol, Belgium.
197. Frasca, B., et al., *Comparative study of Se oxyanions retention on three argillaceous rocks: Upper Toarcian (Tournemire, France), Black Shales (Tournemire, France) and Opalinus Clay (Mont Terri, Switzerland).* Journal of Environmental Radioactivity, 2014. **127**: p. 133-140.
198. Scheinost, A.C., et al., *X-ray absorption and photoelectron spectroscopy investigation of selenite reduction by Fe-II-bearing minerals.* Journal of Contaminant Hydrology, 2008. **102**(3-4): p. 228-245.
199. Chakrabrty, S., F. Bardelli, and L. Charlet, *Reactivities of Fe(II) on Calcite: Selenium Reduction.* Environmental Science & Technology, 2010. **44**(4): p. 1288-1294.
200. Reeder, R.J., et al., *Mechanism of SeO42- substitution in calcite - an XAFS study.* Geochimica Et Cosmochimica Acta, 1994. **58**(24): p. 5639-5646.
201. Aurelio, G., et al., *Structural study of selenium(IV) substitutions in calcite.* Chemical Geology, 2010. **270**(1-4): p. 249-256.
202. Stringfellow, W.T., et al., *Physical, chemical, and biological characteristics of compounds used in hydraulic fracturing.* Journal of Hazardous Materials, 2014. **275**: p. 37-54.
203. MacQuarrie, K.T.B. and K.U. Mayer, *Reactive transport modeling in fractured rock: A state-of-the-science review.* Earth-Science Reviews, 2005. **72**: p. 189-227.
204. Steefel, C.I. and K. Maher, *Fluid-Rock Interaction: A Reactive Transport Approach*, in *Thermodynamics and Kinetics of Water-Rock Interaction*, E.H. Oelkers and J. Schott, Editors. 2009. p. 485-532.
205. Steefel, C.I., et al., *Reactive transport codes for subsurface environmental simulation.* Computational Geosciences, 2015. **19**(3): p. 445-478.
206. Steefel, C.I., L.E. Beckingham, and G. Landrot, *Micro-Continuum Approaches for Modeling Pore-Scale Geochemical Processes*, in *Pore-Scale Geochemical Processes*, C.I. Steefel, S. Emmanuel, and L.M. Anovitz, Editors. 2015. p. 217-246.
207. Pyrak-Nolte, L.J. and D.J. DePaolo, *Controlling Subsurface Fractures and Fluid Flow: A Basic Research Agenda*. 2015, Department of Energy.

208. http://www.mont-terri.ch/. *The Mont Terri Project*. Available from: http://www.mont-terri.ch/internet/mont-terri/en/home/rock_lab.html.
209. Schafer, T., R. Dohrmann, and H.C. Greenwell, eds. *Filling the gaps – from microscopic pore structures to transport properties in shales*. CMS workshop lectures. Vol. 21. 2016, Clay Mineral Society.
210. http://criticalzone.org/shale-hills/. *Shale Hills Critical Zone Observatory*. Available from: http://criticalzone.org/shale-hills/.
211. http://mseel.org/. *The Marcellus Shale Energy and Environment Laboratory* Available from: http://mseel.org/.